UNIVERSITÀ DEGLI STUDI DI PADOVA

DIPARTIMENTO DI INGEGNERIA INDUSTRIALE
CORSO DI LAUREA MAGISTRALE IN INGEGNERIA CHIMICA E DEI PROCESSI INDUSTRIALI

Tesi di Laurea Magistrale in
Ingegneria Chimica e dei Processi Industriali

Design and development of microfluidic platforms to control transport phenomena for biomedical applications

Relatore: Prof.ssa Elisa Cimetta

Laureando: ILARIO ROSSI

ANNO ACCADEMICO 2018 –2019

Riassunto

Per microfluidica si intende quella scienza, sviluppatasi negli ultimi decenni, che si pone come obiettivo lo studio di fenomeni alle scale nano e micrometriche. Il fine è quello di sfruttare il comportamento dei fluidi che, a queste grandezze, sono governati da forze completamente diverse rispetto a quelle che più tipicamente agiscono sulla macroscala.
La rapida elaborazione dei campioni e il preciso controllo dei fluidi, hanno reso la microfluidica un'ottima candidata per sostituire i tradizionali metodi sperimentali in campo biologico. Nel dettaglio, per quanto riguarda questo lavoro di tesi, tale tecnologia viene sfruttata per superare i limiti relativi alle tradizionali culture *in vitro*, come ad esempio i lunghi tempi sperimentali e la difficoltà nel ricreare fedelmente il complesso microambiente cellulare.
Durante questo lavoro di tesi è stata progettata e ottimizzata una piattaforma microfluidica con lo scopo di creare, al suo interno, un gradiente continuo di concentrazione. Tale dispositivo verrà utilizzato per indagare e studiare nel dettaglio il comportamento degli esosomi (vescicole cellulari, identificate come biomarcatori) nella diffusione metastatica del Neuroblastoma, un aggressivo tumore dell'età infantile.
Il dispositivo microfluidico, o micro-bioreattore, dopo un'attenta progettazione, è stato studiato da un punto divista fluido dinamico, al fine di comprendere e verificarne la funzionalità in vista di una sua concreta applicazione in campo biomedico. La produzione segue un processo a due stadi: si è inizialmente prodotto lo stampo tramite l'utilizzo di una microfresatrice e in seguito il micro-bioreattore è stato ottenuto tramite un processo di replicazione dallo stampo. Il comportamento del micro-bioreattore è stato verificato tramite validazioni fluidodinamiche e biologiche per assicurare la sua reale funzionalità.
In parallelo si è studiata e prodotta una configurazione, costituita da una struttura multistrato facilmente implementabile nel micro-bioreattore, che favorisca una rimozione facilitata delle cellule dal dispositivo ad esperimento ultimato, e permetta quindi di effettuare in modo più semplice le varie analisi biologiche sul campione trattato.
Seppur un ulteriore studio sia necessario per risolvere alcuni problemi relativi alla validazione biologica della piattaforma e del sistema facilitato di rimozione, questo lavoro di tesi costituisce un importante tassello per l'avanzamento del progetto di ricerca condotto dalla prof.ssa Elisa Cimetta, con lo scopo di investigare il ruolo degli esosomi nello sviluppo del Neuroblastoma.

Summary

With the word microfluidic we refer to the science, developed in the last couple of decades, which studies transport phenomena at the nano- and microscale. The aim is to exploit the behaviour of fluids that, at this length scale, are governed by different forces with respect to the macroscale.

Among the various fields in which microfluidics has been developed, important studies has been led on biomedical and biological applications. The fast samples analysis and the precise control of fluid flows have made microfluidic a good alternative to the traditional experimental methods. As far as this work of thesis is concerned, this science is used to surpass some of the limitations of traditional *in vitro* cultures, such as the long experimental times and the inability of recreating the complex cellular microenvironments.

During this work of thesis, a microfluidic platform has been designed and optimised, with the aim of reproducing a continuous concentration gradient inside it. This device will be used to investigate and study the behaviour of exosomes (cellular vesicles, identified as bio-markers) on the metastatic diffusion of Neuroblastoma, an aggressive childhood tumour.

The microfluidic device, or micro-bioreactor, after a detailed design phase and before its final production, is studied with computational models to predict its behaviour on a fluid dynamic standpoint, in order to understand and verify its functionality. The production phase follows a two-step process: first, the aluminium master mold is machined using a micromiller, and finally the microfluidic platform is produced via a replica molding process. The micro-bioreactor behaviour it is tested performing fluid dynamic and biological experiments in order to verify it's operating correctly.

In addition, a new configuration formed by a multilayer structure enabling the reversible hydraulic seal, is studied and produced, to facilitate the retrieval of cells form the micro-bioreactor at the end of each experiment, in order to more easily perform post-processing analyses on the cultured cells.

Even if further studies are necessary to solve some problems concerning the success of the cellular culture and the hydraulic seal of the reversible configuration, this work of thesis represents an important step for the successful advancement of the research project, led by Professor Elisa Cimetta, with the overarching goal of investigating the role of exosomes in Neuroblastoma dissemination.

Table of Contents

List of figures

CHAPTER 2

CHAPTER 3

APPENDIX A

Figure A.2 Results of the COMSOL simulation of the μ-bioreactor for case 2: (a) velocity magnitude and (b) cell Reynolds number.

Figure A.4 Results of the COMSOL simulation of the μ-bioreactor for case 1: (a) velocity magnitude and (b) cell Reynolds number.

List of tables

CHAPTER 3

Introduction

Microfluidics is the science that studies the behavior of fluids at the nano and micro scales into microfluidic platforms. This relatively new technology is characterized by precise manipulation and high control of fluids along space and time; furthermore the use of microfluidic device diminish the quantity of reagents and biological material needed, obtaining precise and controllable conditions in the cellular cultures

Considering all these features it is possible to reproduce the cellular microenvironment, and to study in a more realistic way what happens *in vivo*, that is not possible to represent in the traditional *in vitro* models.

For all these reasons the microfluidic platform seems to be a suitable instrument to investigate the role of exosomes, cellular vesicles identified as biomarkers, in Neuroblastoma dissemination and metastasis. Neuroblastoma is an aggressive type of tumor that develops during childhood, witch represents about 8% of all malignancies diagnosed in paediatric patients younger than 15 years of age but is responsible for a disproportionate percentage of paediatric cancer deaths, approximately 15%.

Exosomes are responsible of the communication and the delivery of information between cells and an exhaustive knowledge of their behavior can help to understand how the tumor spreads around the body. This is one of the main field of study of the BIAMET laboratory, where this work of thesis is developed.

The aim of this work of thesis is the design and the development of a microfluidic platform, that could create exosomes' continuous concentration gradients to which cells will be subjected. In fact, the creation of this gradient allows to:

- reproduce *in vitro* what happens *in vivo* thanks to 3D cultures;
- test the effect of exosomes, understanding in which way they are internalized by cells;
- exploit the limited quantity of exosomes that can be extracted from Neuroblastoma cells thanks to the obtainment of high-throughput data.

The platform is firstly designed and its fluid dynamic behavior is simulated using simulation software. Than the master is produced using a micromiller and the platform is constructed via replica molding. Finally the platform is assembled in an irreversible configuration using a glass slide. Some fluid dynamic experiments are performed to validate its behavior and some biological test are carried out to verify whether the device is suitable for cellular culturing or not. The production of the master was possible thanks to the help and collaboration with Professor Marco Sorgato of TE.SI. laboratory, based in Rovigo.

In parallel with the design and production of the microfluidic platform, also called micro-bioreactor, a reversible bonding system is studied. The aim of this system is to promote an

easily removal of cells from the micro-bioreactor after an experiment in order to post process them and to obtain more quantitatively results.

The thesis is formed by three chapters.

In the first one, the state of the art about microfluidics and its main application to the biological and biomedical fields are presented. The techniques and the materials employed to produce the master and the platforms are then reported. Plasma treatment, a technique widely used in this field, is described and explained. Finally, a brief description of Neuroblastoma cancer and of the role of exosomes in its metastasis dissemination process is described.

In the second chapter the materials and the methods used for the design and the production of the microfluidic platform are described. The design of the master, the operation mode and the conditions employed in the fluid dynamic simulations are presented. Then, the production and assembling techniques are described in detail. Finally the validation and biological experiments, including the daily sub culturing procedure, are illustrated.

In the third Chapter the results are presented and discussed. The results of the simulations and of the fluid dynamic validation experiments are shown. Than the cells viability of the irreversible configuration is test and the results are reported. Finally the irreversible configuration is presented and its the hydraulic seal is tested, reporting the results. The outcomes of all these tests, as well as the problems found, are illustrated.

In the Conclusions a brief overview of this work of thesis is presented, focusing on the results obtained, the limitations and the suggestions for a future work.

Chapter 1

State of the Art

1.1 Microfluidics

The term microfluidics refers to the science that investigates the behaviour of fluids at the nano and micro scale. In these dimensions, the amounts of fluids that are processed are small and between 10^{-9} to 10^{-18} litres [1]. Although most of the popular application of microfluidics concerns devices used in chemistry, biology, and medicine, there are also used such as for control systems and heat management, energy generation and display technology [2]. As far as the main applications are concerned, some examples are protein crystallization, proteomics, micromechanical systems, clinical and forensic application, micropumps, sample pretreatement and molecular diagnostic [2]. Another important use of microfluidics is in separation techniques, particularly for nucleic acids, including DNA separation and analysis [2]. For all the biological, chemical and medical applications mentioned above the use of microfluidic devices offers a large number of capabilities such as the ability to use very small quantities of reagents and samples and carry out separations and detentions achieving a high selectivity and resolution with a low cost and short analysis time [1]. These properties of microfluidics technologies have made them attractive candidates to replace traditional experimental approaches [3]. Conceptually, the main idea of microfluidics is that fluids can be precisely manipulated at the microscale using devices built with technologies first developed by the semiconductor industry and later expanded by the micro-electromechanical systems field. These devices are commonly referred to as lab-on-a-chip (LoC) technologies. The phenomena that dominate the behaviour of liquids flowing inside a microfluidic device are measurably different from those that dominate the flow of a fluid at the macroscale. Because of scaling laws, shrinking existing large devices and expecting them to function well at the microscale is often counterproductive. Firstly, it is important to notice that inside a microfluidic device a fluid typically flows in laminar regime, allowing for highly predictable fluid dynamics while turbulent regimes usually characterize macroscale flows. Molecular transport also changes dramatically at the nano and microscale, because convective mixing does not occur, enabling predictable diffusion kinetics. Surface and interfacial tensions are

also dominant at this scale compared to gravity, which has greater effects at the macroscale. These phenomena have been used by researchers to conduct protein and cell sorting, perform nanoreactions for protein crystallization, and passively drive fluids through microchannels. Finally, capillarity, which describes the movement of a fluid through a narrow constriction, has a prominent role at the microscale, allowing fluids to advance in opposition to gravity [3]. Furthermore, the use of optically transparent material to produce microfluidic devices makes them suitable for real-time and high-resolution microscopy: coupling this fact with temporal and spatial control of the physical and chemical environment, microfluidic live imaging can offer insight into processes developing at the nanometer scale. [4]
In summary, the flexibility of device design and the introduction of automated operations, enables to perform complex experiments that improve the accuracy and throughput of biological assays by orders of magnitude [5].

1.1.1 Physics properties of microfluidic devices

Physical phenomena that occur inside a microfluidic device are various and their effects can be competing. The most useful tools to evaluate the relative importance of each phenomenon are dimensionless numbers. Table 1.1 reports the parameters typically used in such analyses.

Table 1.1 *Most commonly used dimensionless numbers; adapted from* [2]

Acronym	Name	Phenomena compared
Re	Reynolds	Inertial/viscous
Pe	Péclet	Convection/diffusion
Ca	Capillary	Viscous/interfacial
Wi	Weissenberg	Polymer relaxation time/shear rate time
De	Deborah	Polymer relaxation time/flow time
El	Elasticity	Elastic effects/inertial effects
Gr	Grashof	Re for buoyant flow
Ra	Rayleigh	Pe for buoyant flow
Kn	Knudsen	Slip length/macroscopic length

To define each of these numbers it is necessary to know the physical properties of the fluids examined, the geometrical characteristics of the devices, and the operative variables (ie. flow rates etc). As far as microfluidics is concerned, the most important parameters and their reference values for a flux of water are reported in Table 1.2.

Among the most commonly used dimensionless numbers, we cite Reynolds, Péclet and the Capillarity number, defined in detail in the following lines.

Table 1.2 *Typical parameters for a flux of water in a microfluidic device; adapted from* [2].

Parameter	Value
Velocity	10^{-6}-10^{-4} m/s
Channel radius	10^{-6}-10^{-4} m
Channel length	$5 \cdot 10^{-3}$-10^{-1} m
Temperature	278 K
Density	1000 kg/m^3
Viscosity	$1 \cdot 10^{-3}$ Pa·s

Reynolds is the most important and meaningful dimensionless number; it gives an indication of the relative importance between inertial and viscous forces. Considering the flow of an incompressible Newtonian fluid in a pipe, the Reynolds number can be defined as:

$$Re \equiv \frac{\rho v d}{\mu} \tag{1.1}$$

where ρ is the density of the fluid, expressed in [kg/m^3], v is the average velocity in [m/s], D is the pipe diameter in [m] and μ is the viscosity of the fluid, usually expressed in [Pa·s]. In a non-tubular pipe, the diameter is calculated as an equivalent diameter, given by the following relation:

$$D_{eq} = \frac{4S}{2P} \tag{1.2}$$

where S is the section of the channel in [m^2] and P is the semi-perimeter [m].
The Reynolds number in microfluidic devices is usually small because the viscous forces overwhelm the inertial ones. It can be demonstrated that, for a tubular pipe, the flow can be considered laminar if Re is less than 2100, for Reynolds between 2100 and 5000 there is a transition from the laminar to the turbulent flow and for Reynolds greater than 5000 the flow can be considered turbulent.

Using the values reported in Table 1.2 Reynolds number can be calculated for a typical microfluidic device, and it results to be between 10^{-6} and 10. The flow is thus laminar: it is highly predictable and it can be described with simpler equations with respect to the turbulent regime. In fact, the turbulent flow is characterized by the presence of eddies which makes unpredictable and instable the flow field.

Equation (1.3) represent the Navier-Stokes equations in vectorial notation used to calculate the velocity field inside a pipe; for a laminar flow of an incompressible fluid they can be easily simplified and solved. The result is known as the Hagen Poiseuille equation (1.4) and it expresses the velocity inside the pipe as a function of the radial position r.

$$\rho \frac{Dv}{Dt} = \frac{\partial v}{\partial t} + (v \cdot \nabla)v = -\nabla p + \mu \nabla^2 v + \rho g \tag{1.3}$$

$$\Rightarrow v = 2V\left(1 - \frac{r^2}{R^2}\right) \tag{1.4}$$

In equations (1.3) and (1.4) $\boldsymbol{v}$ is the vector of the velocity in the three dimensions [m/s], p is the pressure [Pa], $V=Q/A$ is the average velocity [m/s] and R is the radius of the pipe [m].

In Figure 1.1 can be seen the expected parabolic velocity profile along the pipe. According to equation (1.4) the velocity is zero $(v = 0)$ on the pipe wall $(r = R)$ and it assumes its maximum value $(v = v_{MAX})$ in the middle $(r = 0)$.

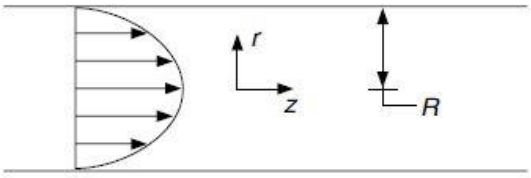

Figure 1.1 *Typical parabolic velocity profile along a pipe*

It is possible to evaluate the pressure drop ΔP along the pipe using the Fanning equation (1.5)

$$\Delta P = 2f\frac{L}{D}\rho v^2 \tag{1.5}$$

where L is the length of the pipe in [m], D is the diameter in [m] and f is the friction factor [adim]. This can be obtained, in the case of laminar flow, as follows:

$$f = \frac{16}{Re} \tag{1.6}$$

Substituting (1.6) in (1.5) gives the following equation:

$$\Delta P = 32\frac{\mu L}{D^2}v = g(v) \tag{1.7}$$

It can be noticed that if the flow regime is laminar the pressure drops are proportional to the velocity filed and not to the square of the velocity as in the turbulent regime. Typical pressure drops can be calculated using values from Table 1.2 and equation (1.7) and the resulting range is between 50 and 1600 Pa. These values show that pressure drops inside microfluidic channels are extremely small.

The second important dimensionless number is the Péclet number that expresses the balance between convection and diffusion, determining which mass transport mechanism is the most

relevant. If Péclet is small ($Pe \ll 1$), the contribution of diffusion to the mass transport is high while if Péclet is high ($Pe \gg 1$), the mass transport is dominated by convection. The Péclet number is defined as follow:

$$Pe \equiv \frac{vD}{D_i}$$

where v is the velocity inside the pipe [m/s], D is the diameter [m] and D_i is the diffusion coefficient of the species i [m^2/s].

Using the values in Table 1.2 and the diffusion coefficient of a small protein in water that is equal to $4 \cdot 10^{-11} m^2/s$, the Pe number results to be in a range between 0.05 and 500, demonstrating the key role played by diffusion in microfluidic devices.

Inside a microfluidic platform, the convective transport is usually smaller than the diffusive one. Although this, on a general perspective, leads to difficulties in mixing, it can be exploited as a great advantage if combined with a careful design of the devices. If there is a difference of concentration of a species i between two sides of a device, with the species moving thanks to diffusion and without significant convection, we can obtain a stable concentration gradient inside the microfluidic device. In detail, the conservation equation for the species i is:

$$\frac{\partial c_i}{\partial t} = -\nabla(c_i v) - \nabla(J_i) + R_i \tag{1.9}$$

The term on the left-hand side represents the variation of the concentration of i with time, the first term on the right-hand side is the convective flux, the second one represents the diffusive flux and the third is the production or consumption of the species during a chemical reaction. Equation (1.9) can be simplified considering that in a microfluidic device there is the predominance of diffusion with respect to the convection, no reaction occurs and the steady state is usually achieved. The resulting equation is:

$$0 = -\nabla(J_i) \tag{1.10}$$

This expression demonstrates that the diffusive flux is constant, assuring constant conditions across the device.

Fick's law describes the diffusive flux [mol/m^2s]:

$$J_i = -\nabla(J_i) \tag{1.11}$$

where D_i is the diffusion coefficient of species i in the medium [m^2/s] and ∇c_i is the concentration gradient of i [mol/m^3].

The Einstein-Smoluchowski equation can be used to calculate the diffusion coefficient of a generic particle:

$$D_i = \eta k_B T \tag{1.12}$$

where η is the mobility of the particle [kg/s], k_B is the Boltzmann constant [J/K] and T is the temperature [K]. In the case of a spherical particle in a viscous fluid, equation (1.12) becomes the Stokes-Einstein equation:

$$D_i = \frac{k_B T}{6\pi\eta r} \tag{1.13}$$

where r is the radius of the particle [m].

As stated above, it is important to notice that a purely diffusive mixing can be desirable or not, depending on the application. Microfluidic chemical reactors allow different solutions to be brought together and mixed rapidly, enabling to probe the kinetics of the reactions, rather than being limited by the diffusive dynamics of the molecules themselves. The opposite problem is faced, however, in sorting and analyzing the products of those same reactions: the faster the mixing, the harder the separation. Controlling dispersion in microfluidic devices, thus, is often of paramount importance. To exemplify let's consider a T junction (Figure 1.2a) in which two different fluids flow alongside each other; the mixing process occurs after a certain time and it is completed at a certain distance downstream the T junction. This process is strictly dependent on the diffusive flux and the diffusion coefficient of the particles involved, and it proves how mixing can occur in absence of convection and in a purely laminar regime. Another example of how the diffusive properties can be used is the case of the membraneless H filter (Figure 1.2b); it exploits the different rates at which tracers with different diffusivities spread across a channel.

Larger products do not have time to diffuse across the channel, and thus remain confined to their initial stream, whereas smaller molecules of interest diffuse across the channel into the

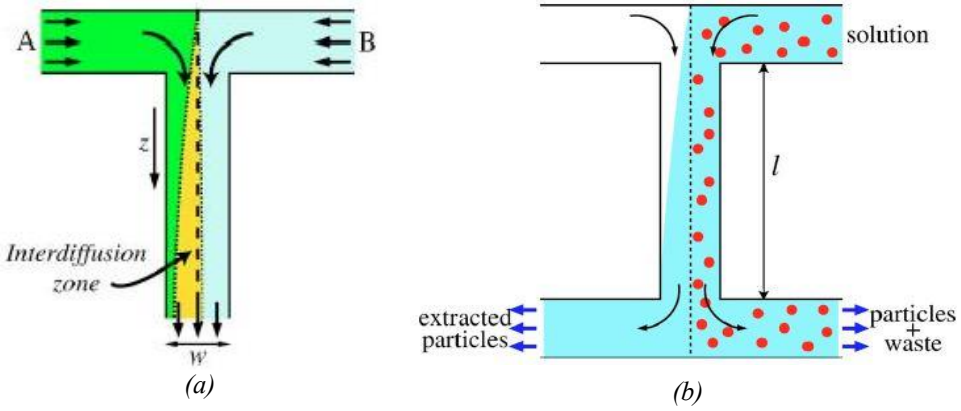

Figure 1.2 *Two microfluidic devices that explain the different diffusion coefficients of the solute: (a) T-sensors and (b) membrane-less filters; adapted from [2].*

neighboring stream. At the outlet, the second stream contains the more mobile species almost exclusively [2].

It is now necessary, to complete a general overview on the most meaningful dimensionless number, to spend some words about the parameter called surface tension γ, even if we will only use miscible fluids in our microfluidic devices. Surface tension can be a fundamental aspect to be considered in systems like T junctions, when used to create controllable droplet emulsions. By injecting water into an oil stream, thanks to the surface tension, the interfacial area between the two liquid phases is minimized forming spherical droplets. Analyzing all the stresses present at the interface, a balance between the viscous and interfacial stresses could be made to obtain the single droplet radius:

$$R \sim \frac{\gamma}{\eta v} h = \frac{h}{Ca} \tag{1.14}$$

where the capillary number [dimensionless] is defined as:

$$Ca \equiv \frac{\mu v}{\gamma} \tag{1.15}$$

The capillary number expresses the competition between the viscous and the interfacial stresses. It is useful to estimate the possibility of creating monodisperse droplets, due to the deterministic nature of microfluidic flows. The presence of a homogenous distribution of droplets has been used to study chemical reaction kinetics on millisecond time and in some applications for protein crystallization. Droplets are advantageous for this sort of study because reagents are not dispersed beyond the boundary of the drop [2].

1.1.2 Biological applications of microfluidics

One of the most important aims of systems biology is to develop a complete understanding of cellular mechanisms by studying the functions of intra and inter-cellular molecular interactions that trigger and coordinate cellular events. However, due to the complexity of biological systems, it is difficult to achieve the required level of precision in system biology experimentation [6].

This limitation is caused by many aspects like the presence of different cell types, of extracellular matrix and the intricate network of molecular and physical factors that activate different signal pathways and regulate cells' functions and fate. Furthermore, the use relatively large operating volumes and the periodic exchange of medium do not allow for the generation of precise spatial and temporal patterns of stimulation. Fortunately, microscale technologies now offer potential for conducting highly controllable and sophisticated experiments at biologically relevant scales, with real-time insights into cellular responses [7].

Moreover, high-throughput experiments are preferred to obtain a quantity of data adequate to describe completely a complex biological system. Therefore, microfluidic devices seem useful instruments, in particular thanks to the following characteristics [2], [5], [7]:

1. Due to the small geometrical dimensions in nano and microscale system, the movement of fluids is laminar, and placement of fluid volumes in the nanoliters-range, picoliter-range and even femtoliter-range is possible.
2. The use of on-chip membrane valves allows precise chemical and physical control of the microenvironment. The doses delivered to the culture can be precisely measured in nanoliters and femtoliters; this represent a significant improvement in precision compared to the traditional manual pipette that can measure microliters at best.
3. It is possible to obtain a precise control of cell numbers and density in a given area or volume; the cells, if required, can also be arranged in a specific position to obtain high-precision experiments.
4. Cells can be organized into three-dimensional geometries in matrices such as hydrogels, allowing culture of cells in structures resembling those in tissues.
5. The small dimensions of microfluidic compartments allow the use of a multitude of individually controllable cell culture chambers on a single device. This facilitates high parallelization of experiments, high throughput of samples and reactions and thus improvement of reproducibility. In addition, the cost of reagents is reduced due to the small amount consumed.
6. The possibility to automate microfluidic cell culture systems gives the possibility to culture cells for several weeks under precisely defined conditions without manual intervention. These automation leads to standardized manipulation, monitoring and sampling of cultured cells and it allows strict adherence to the timing of protocols, which is very important when the time order of magnitude is around seconds or minutes.
7. Microfluidic devices can be constructed using transparent materials providing excellent live cell imaging conditions. In combination with fluorescent live cell imaging, microfluidic cell culture devices therefore allow powerful characterization of a multitude of cellular responses on a single cell as well as population level.

In Table 1.3 are represented the differences between the use of micro and macroscale in biological applications; in particular, the diffusion and the reaction time differ the most, providing a significant reduction in the experimental time.

Table 1.3 *Basic requirements for cell culture, and improvements when microfluidic methods are used; adapted from* [5].

Requirements	Conventional cell culture	Microfluidic cell culture
Control of temperature and gasses	Large fluid volumes prevent fast changes	Small volumes allow dynamic control
Addition of nutrients and removal of metabolites	Infrequent, manual exchange of large volumes	Precisely measured, continuous or transient
Stimulation with drugs/proteins and simultaneous imaging	Usually not feasible	Feasible
Parallelization of cellular assay	Not feasible	High capability for parallelization
Automation of cell culture	Bulky, expensive fluid-handling robots must be used	High capability for automation in compact, inexpensive format
Single-cell manipulation and analysis	Manually involved, inaccurate, low-throughput	Accurate and high-throughput

Even if it seems that microfluidic could be a useful tool to substitute the conventional cell culture methods, we highlight here some of the most common drawbacks of these small devices [4], [5]:

1. The small volumes of media in microfluidic cell culture devices can result in faster consumption of nutrients and in an increase of the concentration of metabolites or secreted molecules. A consequence is that the small volumes might necessitate more frequent replacement of media or addition of nutrients. Figure 1.3 shows the different dimensions between the conventional cell culture technique and a microfluidic device.
2. The high surface area to volume ratio of a microsystems causes not only heat dissipation from inside the channel to the outside but it can also enhance surface

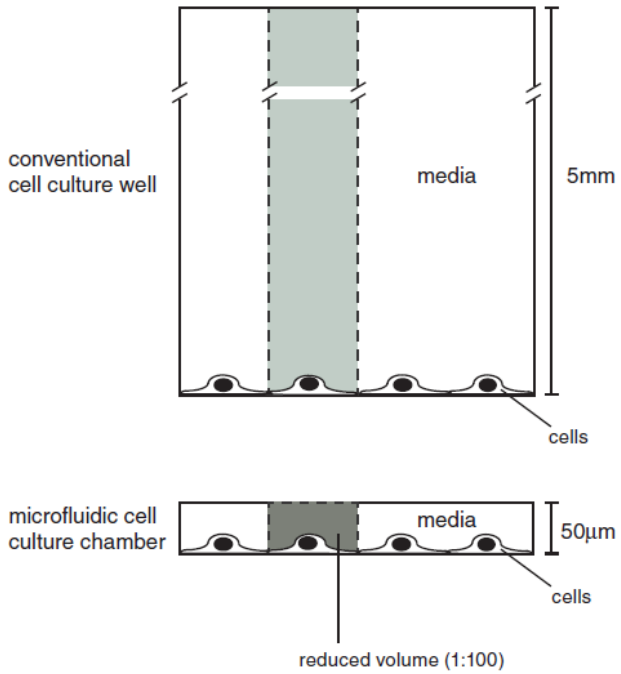

Figure 1.3 *Comparison between the conventional cell culture technique and a microfluidic device; adapted from [5].*

adsorption losses. Careful consideration of surface treatments must be made.

3. Processing large volumes of fluid requires long time because of the small dimensions and very low volumetric flow rates that are generally used in microfluidic devices. For example, a channel with a 10 μm diameter would take ~1,000 minutes for a 1 ml volume to pass, compared with less than 1 minute in a 1 mm diameter channel at the same applied pressure. For high-volume applications, it may be more appropriate to consider mesofluidic approaches.
4. Microchannels may be clogged by debris or bubbles, and this problem can make the experiment fail.
5. Conventional pipettes deliver microliter volumes, whereas microdevices typically analyze nanoliter volumes. This means that the major part of the sample will potentially be wasted.
6. Specialized requirements: microfluidic approaches may require specialized instrumentation, expertise in engineering design and non-conventional data interpretation strategies, particularly at the earliest stages of device development.
7. It may result difficult, or even impossible, to compare the results of the experiments with published and confirmed studies, because of the lack of accepted standards and controls. The new studies and researches can be slowed down by this limitation.

1.2 Microfluidic technologies

The design of a microfluidic device is strictly correlated with the final application of the platform. It is then important to take into consideration all physical and chemical phenomena listed above to obtain the desired result. Typically, a microfluidic platform used for biological experiments consists of a series of microchannels arranged in such a way to obtain the desired fluxes and overall performances. The device can be designed to include a variety of additional elements, such as pumps, valves and mixers. The network of microfluidic channels inside the microfluidic device is connected to the outside by inputs and outputs ports punched through the chip. Through these holes, using micropipettes or a syringe pump, the fluids are pumped inside and outside the device.

There are many materials that can be used for biological applications, like silicon-based organic polymers, glass, or metals; each one is chosen with respect to the specific application.

Overall, the most used materials for biological devices is Polydimethylsiloxane (PDMS), a silicon rubber, mainly thanks to its high compatibility with the cellular environment. Its characteristics will be explained in detail in the following paragraphs.

As far as fabrication methods are concerned, currently used techniques include micromachining, soft lithography, embossing, *in situ* construction, injection molding and laser

ablation [8]. Each technique has different advantages and disadvantages, and the most suitable one depends on the specific function.

Microfluidic devices can be divided into two categories, monolayer and multilayer platforms, with respect to the number of functional layers that they possess:

- Monolayer platforms are formed by a single layer of polymer that is usually attached to a glass slide or to another polymer, to obtain hydrodynamic seal. Their design is quite simple with respect to the multilayer ones; they are among the most used microfluidic devices.
- Multilayer platforms are formed by at least two layers, attached to each other and to a support, to obtain more complex systems, with different features with respect to the monolayer ones. Their design is more complicated, since each individual layer is deigned to obtain specific elements, like valves or pumps. Usually some markers are present in each layer to guarantee the perfect alignment between each layer. These platforms allow to use automatized systems and to obtain more complex and useful structures. Unfortunately, the greater complexity of multilayer platforms might lead to some drawbacks; the most common is the phenomenon of lamination. It consists on the detachment of the different layers of a platform from another or from a glass slide; this is due to a non-optimal adhesion of the different layers during bonding or excessive operating pressure used during operation procedures and it causes the breakdown of the platform.

1.2.1 Design and production of the master

In most cases, a microfluidic device is produced using a master that can be made by different materials such as metals or resins. The master is usually designed in a 2D and 3D-CAD environment. In the following paragraphs we describe two techniques employed to prepare these masters: photo lithography and micromilling.

1.2.1.1 Photolithography

Photolithography is a fast and cheap technique used to produce masters for microfluidic devices. It is a patterning technique extremely important because it allows creating a mold that can be used to reproduce micrometric structures on elastomeric materials.

To obtain an excellent mold with this technique it is necessary to carry out the master production process in a clean room, an environment completely free from dust and any other type of contaminants that can compromise the successful obtainment of the desired structures. The main steps of the procedure are as follows:

1. A silicon wafer is accurately cleaned to remove every contaminants from the surface and dried to remove humidity to facilitate the adhesion of the photoresist (a photosensitive epoxy resin) (Figure 1.4*a*)

2. A layer of photoresist is deposited over the silicon wafer and homogenized with the help of a spin coater to obtain the specific thickness. (Figure 1.4*b*)
3. A photomask, an acetate film with the print of the desired geometry, is positioned over the photoresist; then the wafer is exposed to UV light for a certain time and only the desired zones of the photoresist crosslink (Figure 1.4*c*)
4. After that, the photomask is removed and the wafer is treated with a series of solvents to remove the non-cross-linked photoresist obtaining the mold structure.(Figure 1.4*d*). The master is then harden to fix the photoresist and to make the master more resistant. At this point, the master can be employed to produce the platform via the replica molding process[8].

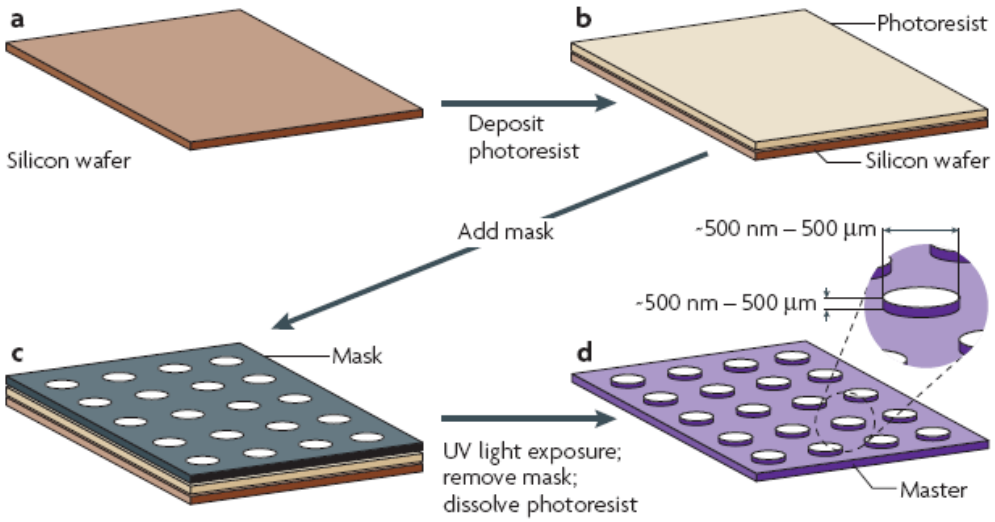

Figure 1.4 *Main steps of photolithography technique to fabricate a microfluidic master: (a) Pretreatement of the silicon wafer; (b) Deposition of the photoresist on the silicon wafer; (c) Deposition of the mask; (d) Exposure to UV light and removal of the non-cross-linked photoresist; adapted from* [25].

Two different types of photoresist can be used depending on the specific geometry: positive and negative]. They differ in the obtainable heights and shape of the section of the channels and in the photolithography workflow. This is due to their different chemical composition and especially their different behavior when exposed to the UV light. A positive photoresist polymerizes only in the regions that are not exposed to the UV light, while a negative photoresist crosslinks where directly exposed to UV. Figure 1.4 shows the procedure for a negative photoresist, and we can see that the region covered by the black areas of the photomask do not polymerize and they are removed.

Whit this technique it is possible to obtain microfluidic structures with width and height between 500 nm and 500 µm.

Within the soft lithography technique, PDMS itself can be used as a soft mold for an additional process of replica molding and thus allowing using a wider range of materials, like agarose or agar.

Other soft lithographic techniques, like capillary molding, microcontact printing and microtransfer molding are used; the choice depends on the materials used and on the design of the microfluidic device.

1.2.1.2 Micromilling

Micromilling is used to produce rigid masters; it allows to obtain precise structures with a precision of 1-2 microns. Micromilling consist in obtaining a well-defined structure milling a block of metal, usually Aluminum, or of another polymer. A micromiller is used to mill the starting block; this machine supports very small tools that allow obtaining the detailed design specifications. The main advantage of this technique is that the obtained master is resistant, it does not modify its dimensions during the replica molding process, and it can be employed at high temperature. On the other hand, one of the main issues is the optimization of the working parameters: the cutting forces that are generated during the production can create deflections and defects, which entity is comparable with the dimensions of the device. The right choice of the cutting parameters allows to finely control the cutting forces. The master is compatible with the standard process of replica molding with PDMS, and can be cured at high temperatures. Thanks to the process of replica molding, using an aluminum master, a virtually infinite number of PDMS devices can be produced with invariant dimensions between them.

1.3 Microfluidic platforms

As described earlier, microfluidic platforms are mainly produced through a replica molding process, starting from an existing master and using a polymer (usually PDMS) to replicate the device. We report here a short summary about PDMS properties and its application technique such as the replica molding process and the adhesion techniques via plasma treatment.

1.3.1 PDMS

Silicone is a synthetic polymer whose backbone is a repeating chain of $Si-O$ molecules with various organic groups attached to the silicon. The silicone termed polydimethylsiloxane $[(CH_3)_2Si-O]$, abbreviated PDMS, has two methyl groups attached to the silicon. Its chemical structure is reported in Figure 1.5.

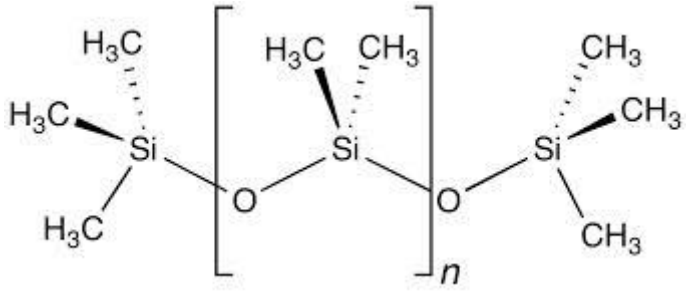

Figure 1.5 *Polydimethylsiloxane (PDMS) chemical structure; adapted from* [26]

PDMS has been widely used to produce microfluidic devices; in fact it can be easily molded to create complex fluidic circuits, using replica molding techniques, making prototyping relatively simple and cost effective. [9]
Its primary advantages over other substrate materials include low cost, fast simple fabrication and optical transparency through the visible spectrum down to 240 nm. Other characteristics of the cured polymer are listed:

- Biocompatibility;
- Low autoflorescence;
- Gas-permeability, that allows O_2, CO_2 and N_2 to permeate across the material and reach the cell culture;
- Non-permeability to water;
- Hydrophobicity;
- High-resolution.

However, different issues can be found in the application of PDMS to microscale cell culture systems [5]:

- PDMS is a hydrophobic and porous material, which results in the undesired absorption of hydrophobic molecules such as lipids or small molecules from culture media into PDMS. To maintain stable cell culture conditions and to reduce the effects of absorption into PDMS, regular replacement of culture media is necessary. Pretreatement of PDMS devices with sol–gel chemistry can reduce small-molecule absorption.
- Small volumes of media in microfluidic cell culture devices can result in faster consumption of nutrients and in an increase of the concentration of metabolites or secreted molecules, especially compared to conventional cell culture techniques. Although these small volume effects need to be carefully considered when designing experimental setups, they arguably reflect physiological conditions of cells or cell-populations in tissues more appropriately than cells that are cultured in larger volumes. However, the small volumes might necessitate more frequent replacement of media or addition of nutrients.
- PDMS is hydrophobic and it has high porosity and permeability to gasses and fluids; these properties can result in rapid evaporation. This effect can be avoided or at least limited by placing the microfluidic device in an environment with high humidity, for example, by building on-chip media reservoirs, or by using incubators connected to a humidifier. Modern incubators allow also control of temperature and concentration of oxygen and carbon dioxide.
- PDMS that is not complexly cured could be toxic to cells; this toxicity is more pronounced for PDMS mixture of base and curing agents out of the standard

volume/volume ratio, usually used in multilayer platforms. To avoid this problem, chips should be baked at the correct curing temperature for the necessary time, which depends on the curing temperature itself. PDMS devices can also be autoclaved to improve biological compatibility.

- Typically, cells do not attach to PDMS; to avoid this limitation the PDMS surface can be coated with proteins such as fibronectin, or various mixtures such as laminin or matrigel.

Two types of PDMS are commonly used by researchers to fabricate microfluidic chips: RTV-615 from Momentive Materials and Sylgard 184 from Dow-Corning; the second one is the PDMS used in BIAMET laboratory. PDMS is prepared mixing two solutions: a base and a curing agent usually mixed 10:1 volume/volume. Their compositions are dimethylsiloxane oligomers with vinyl-terminated end groups ($> 60\%$), silica filler (dimethylvinylated and trimethylated silica, $30-60\%$), tetra (trimethylsiloxy) silane ($1-5\%$) and ethylbenzene $<$ (1%) fot the base and a cross-linking agent (dimethyl methylhydrogen siloxane, $40-70\%$) and an inhibitor (tetramethyl tetravinyl cyclotetrasiloxane $1-5\%$) for the curing agent [9]. Since during the mixing process a large number of bubbles forms, they must be removed with a vacuum desiccator. The degassed mixture, poured on the rigid master, is finally cured either at room or at higher temperatures. In are reported some curing temperature and the time needed to obtain a completely cured PDMS.

Table 1.4 are reported some curing temperature and the time needed to obtain a completely cured PDMS.

Table 1.4 *Recommended curing temperatures [°C] and times for PDMS Sylgard® 184; adapted from [10].*

Temperature [°C]	Curing time
25	48 h
100	35 min
125	20 min
150	10 min

The main characteristics of PDMS prepared with a base and curing agent ratio of 10:1 are reported in Table 1.5:

Table 1.5 *Properties of PDMS prepared with the Sylgard® 184 (Dow Corning) kit; adapted from [12].*

Property	Value
Density	965 kg/m^3
Viscosity (base)	5.1 Pa·s
Viscosity (mix)	3.5 Pa·s
Thermal conductivity	0.27 W·m^{-1}·K^{-1}
Pot life (at 25°C)	90 min

Melting point/Boiling point	N/A (it vetrifies)

The curing temperature also influences mechanical properties of the PDMS such as the tensile strength, the compression strength and the hardness. Some tests taken at different temperature (25°C, 100°C, 125°C, 150°C and 200°C) on Sylgard 184 PDMS from Dow-Corning shows interesting results. Regarding the tensile strength the stress/strain curves display the typical linear elastic region up to stain values of 40% (Figure 1.6a) followed by a nonlinear region before failure. The data indicates that the maximum strain is inversely proportional to the curing temperature. The Young's Modulus for the linear elastic region is linearly dependent with the curing temperature: if the curing temperature increase the Young's Modulus increase linearly. This behavior is shown in Figure 1.6b.

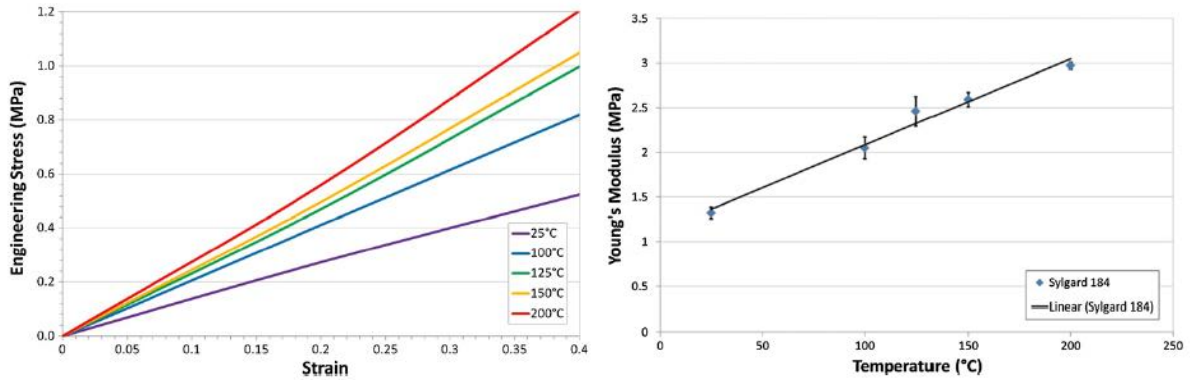

(a) (b)

Figure 1.6 *(a) Averaged tensile engineering stress/strain curves up to 40% strain for PDMS samples cured at different temperatures; (b) Relationship between curing temperature PDMS and the resultant Young's modulus. Adapted from* [10].

As far as the compression strength is concerned, an analogue series of tests have been carried out and are available in literature. Looking at the stress/strain curves in Figure 1.7*a* the linear elastic region goes up to stain value of approximately 55% and it is followed by a nonlinear region before failure. Deriving the compressive modulus (Ec) it can be noticed how it reduces

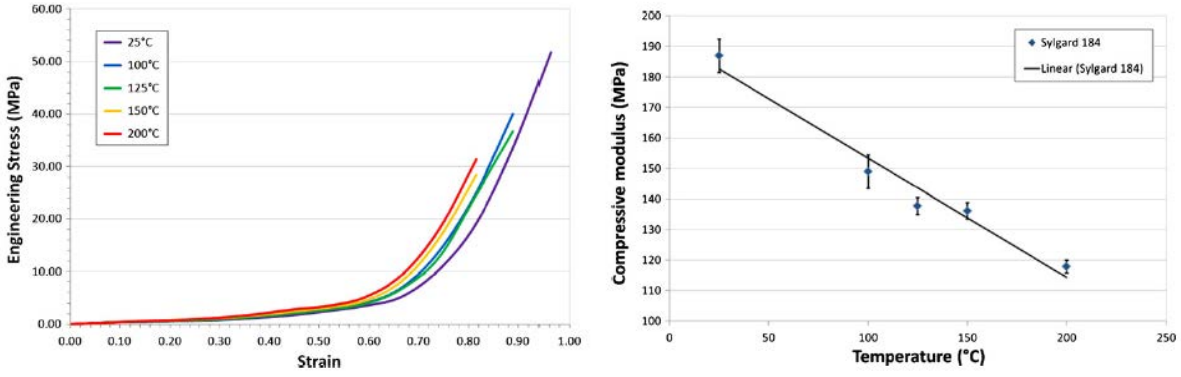

(a) (b)

Figure 1.7 *(a) averaged tensile engineering stress/strain curves up to 40% strain for PDMS samples cured at different temperatures; (b) relationship between curing temperature PDMS and the resultant compressive modulus. Adapted from [11].*

linearly with increasing curing temperatures. (Figure 1.7b)

The hardness of the cured PDMS has been tested and the result is that it varied linearly with increasing curing temperature. Its behavior is shown in Figure 1.8.

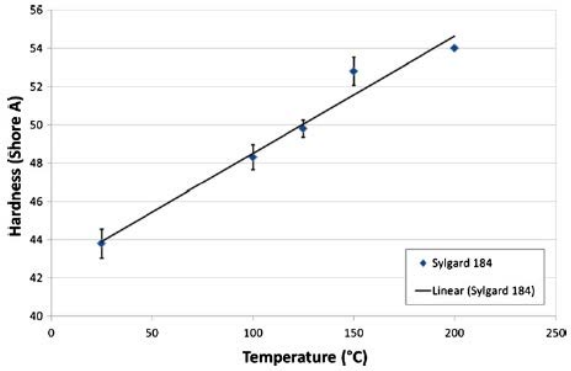

Figure 1.8 *Relationship between the curing temperature of the PDMS [°C] and the resultant hardness [Shore A]; adapted from [11].*

As far as the use of PDMS in microfluidics application in concerned it is fundamental to describe more in detail the replica moulding process, that is the most use technique employed to produce PDMS microfluidic devices.

1.3.1.1 Replica molding

Replica molding is a process that is common with different techniques, in which a master is used to produce microfluidic platforms. The fluid polymer, usually PDMS, is poured on the master and reticulated at the right temperatures for a defined time. After the curing, PDMS can be easily removed from the master to obtain the microfluidic layer. In Figure 1.9 are shown the two described steps to obtain a PDMS microfluidic device.

The device molded in PDMS might be sealed to a glass slide, or to another layer of PDMS, through a plasma treatment that allows the creation of permanent bonds between the two layers.

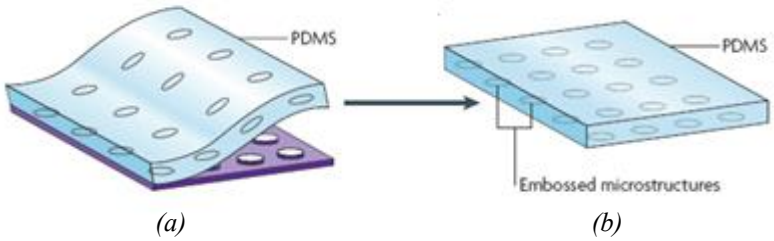

Figure 1.9 *Replica molding of PDMS: (a) Molding of the PDMS over the rigid master; (b) Removal of PDMS layer from the master; adapted from* [25].

1.3.1.2 Plasma treatment

Plasma is the fourth state of matter; it is a distinct processing medium used for surface treatment and surface modification. With the word plasma, we refer to a partially ionized gas consisting of electrons, ions and neutral atoms or molecules. Although the plasma electrons

are at a much higher temperature (around 104 K) than the neutral gas species, the plasma as a whole is at near-ambient temperature. Its density is around 10^{10} cm^{-3}. Plasma can be created either in inert atmosphere or with air; it is generated when a radio frequency oscillating electric field is generated in the gas, either using capacitive plates or through magnetic induction. When pressure is sufficiently low, the combined effect of elastic scattering of the electrons with neutral atoms or field lines and the electric field acceleration of electrons leads to heating of the electrons. When electrons gain kinetic energy in excess of the first ionization threshold in the neutral gas species, electron-neutral collisions lead to further ionization, yielding additional free electrons that are heated in turn. [11][12]

Plasma treatment has a lot of advantages [11]:

- Plasma treatment affects only the near surface of a material without altering its bulk properties;
- Plasma forms at near-ambient temperature, minimizing the risk of damage to heat-sensitive materials;
- Depending on process gases and usage configuration, plasma treatment can be used to clean, activate, or chemically modify surfaces;
- Plasma treatment can be applied to many different materials as well as complex surface geometries, including semiconductor wafers, glass slides and coverslips, oxide and metal nanoparticles, fibrous scaffolds and polymer fibers and porous membranes;
- The energy of plasma electrons and ions is sufficient to ionize neutral atoms, generate excited states in atoms or molecules, break molecules apart to form reactive radical species and locally heat the surface.

Plasmas can interact with and modify a surface through several mechanisms and the most important, as far as this work of thesis is concerned, is surface activation.

Plasma surface activation involves the creation of chemical functional groups on the surface of the material. In particular, during PDMS and glass plasma treatment, as reported in Figure

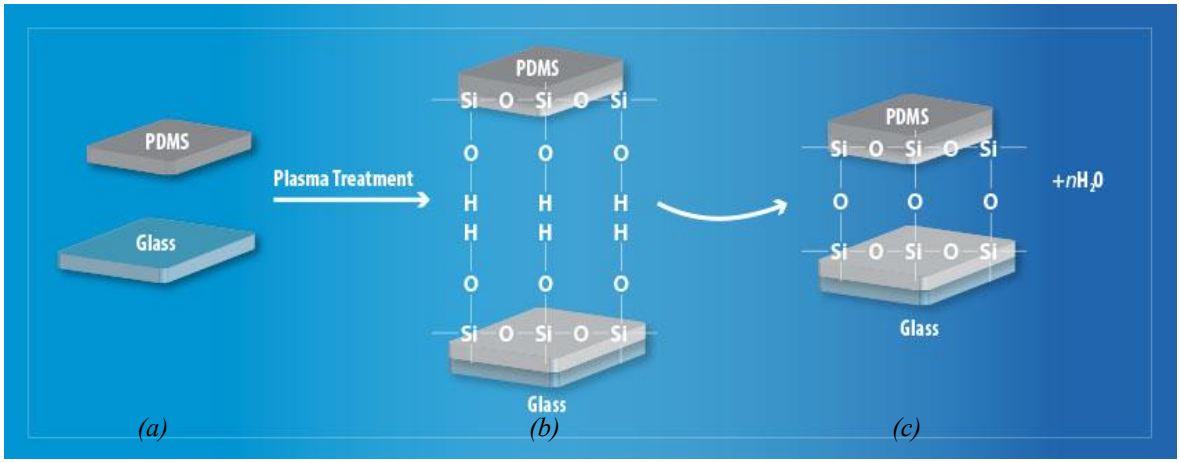

Figure 1.10 *Steps of plasma treatment for attaching a PDMS surface over a glass slide: (b) Activation of PDMS and glass' surfaces through plasma and (c) the creation of a covalent bond between the two surfaces; adapted from* [13].

1.10 the plasma reactive molecules generate silicon atoms with one missing electron on the surface. These silicon bonds combine with the hydrogen atoms create silanol ($SiOH$) groups both on the PDMS and on the glass slide's surfaces, making them hydrophilic. Then, when the plasma-activated surfaces are put into contact, each charged molecule forms a covalent connection Si-O-Si between the two. The hydrophilicity of the surfaces lasts approximately half an hour [13].
The main drawback in the use of plasma treatment in microfluidic device for biomedical application is that it must be done before seeding the cells inside the platform. In fact, the plasma, energetic and reactive, can damage the cells. To overcome this problem the device is usually punched to obtain seeding doors and inlet and outlet holes to easily insert the cells, with the help of a micropipette, after the plasma treatment.

1.4 Neuroblastoma

Neuroblastoma (NB) is a childhood solid tumor that originates in early nerve cells (called neuroblasts) of the sympathetic nervous system [14]. The overall incidence of neuroblastoma is 1 case per 100,000 children in the United States, or about 700 newly diagnosed patients per year. Neuroblastoma represents about 8% of all malignancies diagnosed in paediatric patients younger than 15 years of age but is responsible for a disproportionate percentage of paediatric cancer deaths, approximately 15% [15].
Cancers can spontaneously regress or mature, or display an aggressive, therapy-resistant phenotype. Increasing evidence indicates that the biologic and molecular features of neuroblastoma significantly influence and are highly predictive of clinical behaviour. Because of this, neuroblastoma has served as a paradigm for biological risk assessment and treatment assignment. Most current clinical studies of neuroblastoma, base therapy and its intensity on a risk stratification that takes into account both clinical and biologic variables predictive of relapse. On the other hand, the complex and interacting molecular mechanisms that are involved are yet not completely understood nor defined, mostly because of the lack of appropriate means to study them.
Neuroblastoma is characterized by the ability to "communicate" with nearby cells as well as distant organs. Micro-environmental cues are strong effectors of such communication and play a key role in regulating tumour progression.
Cell communication is essential for tumorigenesis: individual tumour cells must interact with each other and host cells to survive, progress and metastasise. Through inter-tumour communication, a heterogeneous population of cells can co-operate and advance in a hostile environment. It is becoming increasingly clear that tumour-derived Exosomes (a form of endosome-derived extracellular vesicle) play an important role in this communication process [15].

1.1.1 The role of Exosomes in cancer metastasis

Exosomes are 40–200 nm vesicles constitutively secreted by cells of non-haematopoietic origin like epithelial cells (intestinal epithelial cells), astrocytes, neurons, melanocytes, mesothelioma cells, adipocytes, fibroblasts and tumour cells and sourced from numerous body fluids including plasma, serum, saliva, amniotic fluid, breast milk and urine [16][17]. They have been shown to exert their biological functions by horizontal transfer of their mRNA, miRNA or protein content to recipient cells by direct contact between Exosome surface molecules and recipient cells [17].

Exosomes play an important role in cancer progression, metastasis, and therapeutic efficacy.

Several studies have demonstrated that exosomes are involved in initiation, growth, progression and drug-resistance of cancers; exosomes interact with the microenvironment by transferring oncogenic proteins and nucleic acids. Moreover, exosomes are able to promote cancer angiogenesis and metastasis by aiding in the epithelial-to-mesenchymal transition and formation of the pre-metastatic niche.

The role of exosomes in cancer development is of particular interest to oncologists because cancer cells secrete at least 10-fold more exosomes than normal cells, but the mechanism and the signals that induce this form of communication are yet poorly understood.

To understand the role of exosomes as biomarkers, pure exosomes samples are required; even if it is not easy, different methods are employed to isolate exosomes, like ExoQuick precipitation and ultracentrifugation (UC) [16].

1.5 Motivation and aim of the thesis

It is now quite clear how microfluidic might be considered a promising science and how microfluidic devices can be used to recreate in-vitro what usually happens in-vivo. A specific application can be the study of Neuroblastoma and of the role of exosomes in its metastasis: engineering knowledge can be coupled with biomedical expertise, to obtain a deeper comprehension of this very aggressive disease. In particular, microfluidic devices can be employed to create concentration gradients at the steady state and to carry out high-throughput and highly controllable experiments with the aim of investigate how exosomes are internalized by cells. Moreover, the use of microbioreactors and microscale technologies exploiting classical engineering principles would solve the limitations of the existing in vitro models used to study Neuroblastoma derived exosomes.

The work behind this thesis consists in the design and validation of a microfluidic device, capable to generate a steady state concentration gradient to test the effects of exosomes on local and distant microenvironments. After a first part of design and fluid dynamic simulations, the platform master has been constructed, in collaboration with Te.Si., a laboratory of micro and nano machining of the Department, located in Rovigo. Then, after the

production, the microfluidic platform has been fluid dynamically validated and its biological compatibility has been tested, using HEK-293 cells. The final step would be testing its functionality with Neuroblastoma Exosomes to observe how cells internalize them. In parallel, it has been designed and developed a membrane-based vacuum system for the reversible sealing of the micro-bioreactor. This is fundamental as it enables to remove easily the sample of cells for post processing steps, after the conclusion of the experiments. This layer facilitates the attachment and the removal of the microfluidic device from the glass slide, which is not possible if plasma technique is used.

Even if the design should be improved and the design of experiments might be optimized, it is clear how this project provides an important opportunity to advance the understanding of the role of exosomes in the Neuroblastoma dissemination.

Chapter 2

Materials and methods

This Chapter deals with the design of the microfluidic platform and of the vacuum system layers. We will describe the detailed procedure used to produce the masters, and all the testing steps involved in the production chain, starting from the fluid dynamic simulation and ending with the cellular validation.

2.1 Gradient generators

2.1.1 Design

The design of the microfluidic platform originates from a modification of an existing device studied in a previous work of thesis. The overall dimensions of the device are the same, but the internal geometry has been changed. The most important constraint is that the device has to be attached to a 76x26 mm glass slide, thus determining its maximum size. Moreover, the design must satisfy the rules of thumb concerning design of microfluidic devices [18]:

- The "working area" should be enclosed within walls in order to ease manual operations such as cutting the polymerized PDMS layer with the desired dimensions.
- The minimum spacing between different structures (not between channels) has to be not less than 2 mm.
- No structure can be fabricated having an aspect ratio lower than 1:10 (height:width); i.e. if the height is equal to 150 μm, the maximum width of a generic structure must be equal to 1.5 mm. Structures with lower aspect ratios are prone to collapse (Figure 2.1). If the device does not require any microvalves inside it, it is not as prone to collapse and lower aspect ratio can be used.

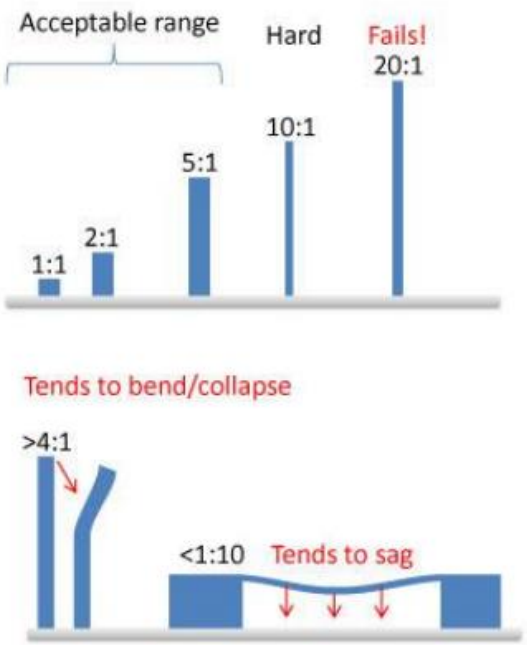

Figure 2.1 *Examples of acceptable and difficult aspect ratios using PDMS features. Adapted from* [27].

- Largest aspect ratios possible for rectangular structures is approximately 1:1 (height of feature : width of feature). For features which are very close together the largest aspect ratio is 1.5:1 (height of feature : spacing between features).
- When a multiple layer platform is designed it is fundamental to add alignment markers to facilitate correct positioning of the different layers.
- It is extremely useful to mark the area where the inlets and outlets of the platform has to be punched, to guarantee a high degree of standardization on the production chain.

The 3D design of the platform is done with Solidworks® while the first 2D design is usually made using AutoCAD®.

2.1.2 COMSOL Multiphysics® simulations

All fluid dynamic simulations are based on COMSOL Multiphysics® modelling software. COMSOL Multiphysics® is organized in modules, which are selected to add or remove specific physics interfaces to the system. To analyze the behavior of the microfluidic device, the velocity and concentration profiles inside the reactor are simulated. COMSOL Multiphysics® allows working on both 2D and 3D domains, but to better describe the properties and the profiles inside the device only 3D geometries are studied.

Operatively, physics that are added to this simulation are:

- the laminar flow of a single-phase incompressible fluid, to describe fluid motion inside the channels;

- the transport of a diluted species, to simulate the convective/diffusive behavior of a generic species *i* inside the platform.

The fluid inside the micro-bioreactor is assumed to be water, since its physical properties are the same as the ones of the solutions used during the experiments.

2.1.2.1 Laminar flow

Navier-Stokes equations describe the laminar flow of a single-phase fluid and they represent the conservation of mass, momentum and energy. These equations are solved numerically considering that the fluid is Newtonian, the density is constant (since temperature is almost constant thanks to the use of cell culture incubators), and that the no-slip condition applies to the walls. The problem is analyzed at the steady state and some initial conditions are required:

- temperature; set equal to 37°*C,* that is the temperature inside the incubator*;*
- inlet medium velocity, that changes with the volumetric flow rate;
- outlet pressure, set equal to 0 *barg*;

With the previous set of conditions, it is possible to obtain the pressure and velocity profiles inside the reactor and to derive, using the correct tool, the Re distribution, to verify if the requirement of laminar flow is satisfied.

2.1.2.2 Transport of Diluted Species

The *Transport of Diluted Species* module has the equations, boundary conditions, and rate expression terms for modelling mass transport of diluted species in mixtures, solutions, and solids, solving for the species concentration. This interface is applicable for solutions, either fluid or solid, where the transported species have concentrations at least one order of magnitude less than the solvent, such as in the case analyzed. While the diffusive term is always included in this module, the convective term is active by default but can be excluded by the user. The velocity term is calculated by coupling this physics interface with the laminar flow. The interface supports simulation of transport by convection and diffusion in 1D, 2D, and 3D as well as for axisymmetric models in 1D and 2D.

The parameters that must be defined are:

- the diffusion coefficient;
- the physical properties of the species that flow inside the platform;
- the initial concentration *c* (at the inlets) of the species.

Since the solution is assumed to be extremely diluted, only the diffusion coefficient of the solute is needed.

2.1.3 Production of the master

The master was produced in the Te.Si. laboratory, in Rovigo, in cooperation with Professor Marco Sorgato using standard micromilling technique. The miller used in is the Kugler MICROMASTER® 5X (Figure 2.2), a high precision machining center, specifically designed and optimized for micromachining and micro-structuring, supplied with 5 simultaneous axes of motion. The base of the unit is made of solid, fine-grained granite, which guarantees the highest long-term thermal and mechanical stability and effectively eliminates vibrations in combination with passive air friction damping elements [19].

Figure 2.2 *Kugler MICROMASTER® 5X micromiller used in T.E.S.I. laboratory in Rovigo; adapted from* [19].

As explained in paragraph §1.2.1.2, it is fundamental to choose the right set of parameters to obtain an highly precise result.

Starting from the 3D-CAD design of the master, developed using SolidWorks®, tools of different dimensions are selected, and the miller is prepared:

- the Aluminum block is fixed on a support;
- the tool is settled and rotated for 10 minutes, to increase its temperature and stabilize its dimensions;
- the zero of the machine is set up;
- the velocity is set to specific values for both the outer surface and the platform;
- the machine is started, and the block is milled. (Figure 2.3)

Figure 2.3 *The milling of the microfluidic platform mold.*

The end mills used for this procedure were a 3mm tool for the outer surfaces, a 2mm tool for the lateral channels, the central chambers and the alignment markers and a 0.15mm tool for the microchannels.
After milling, the master is immersed in ethanol and cleaned in an ultrasound bath.

2.1.4 Metrological characterization of the master

Some optical tests are conduced to estimate the precision of the milling procedure. This is important since variations in the heights of the structural elements may hinder proper attachment of the micro-bioreactor to the glass slide after plasma treatment or led to a modification in the fluid dynamic behavior of the platform. In particular, the measures of interest are the height of the different elements both considering the relative dimension between design elements that are supposed to be at different height and other ones that are supposed to be all at the same height.. The measurements are done using a 3D optical profiler (Sensofar® S Neox, Figure 2.4), with the possibility of employing three modes [20]:

- Confocal Scanning, a technique that utilizes an aperture at the confocal plane of the objective, used to capture 3D and 2D images of the object;
- Optical Interferometry, that exploits the path difference between light reflected in the two arms of the interferometer to yield spatial interference pattern, that contains information on the surface topology of the sample;
- Focus Variation, that scans the entire sample to obtain continuous images, varying continuously the focus and building up the image.

The Focus Variation mode is used for all heights measurements following the procedure described below:

- the whole area of interest is roughly focused with a 5x objective;
- the different specific interest areas are selected with a 20x objective;

Figure 2.4 *Sensofar® S Neox optical profiler used in T.E.S.I. laboratory in Rovigo; adapted from* [20].

- on each area, the focus is manually changed to set the upper and the lower planes, between which the analysis is carried;
- the analysis is started, and the relative heights between the two planes selected are studied.

2.1.5 Production of the PDMS micro-bioreactor

The microfluidic platform is produced using the replica molding process. The material used is PDMS Sylgard® 184 (Dow Corning), provided as a two-part kit (DOWSIL™ 184 Silicone

Figure 2.5 *PDMS Sylgard® 184 (Dow Corning). Base and curing agent.*

Elastomer kit): the silicone elastomer base and the curing agent (as shown in Figure 2.5.).
The main production steps are:

1. Weighing of the base and curing agent in a proportion of 10 parts of base and 1 part of curing agent, inside a disposable plastic container;
2. Energetic mixing for two minutes of the base and the curing agent in order to create a homogeneous mixture. During this step, a large quantity of bubbles is formed inside the mixture;
3. Removal of the bubbles thanks to a desiccator (Figure 2.6) connected to a vacuum pump: the plastic container with the mixture, covered with aluminum foil to avoid dust contamination, is placed inside the desiccator chamber; the pump is switched on to create vacuum inside the chamber and thus allowing the bubbles to emerge and expand. After approximately 10 minutes, the pump is switched off and the valve of the desiccator is opened to gently return to atmospheric pressure. This step makes the bubbles on the surface of the mixture blow up. The procedure is repeated (usually 4 or 5 times) so that all the bubbles are removed;

Figure 2.6 *Desiccator connected to the vacuum pump used in the BIAMET laboratory.*

4. Cleaning of the master with a flow of compressed air to remove dust particles from its surface;
5. Pouring of the desired PDMS quantity on the aluminum master, and removal of additional bubbles that can create during the pouring step, with the same procedure of step 3 (Figure 2.7);
6. Curing of the PDMS on the master at 65°C for 75min, inside an oven. This temperature is set based on the provided values listed in are reported some curing temperature and the time needed to obtain a completely cured PDMS.
7. ***Table 1.4***;
8. Extracting the master from the oven and waiting until it reaches room temperature;

9. Removal of the cured layer from the rigid master, carefully using a scalpel;

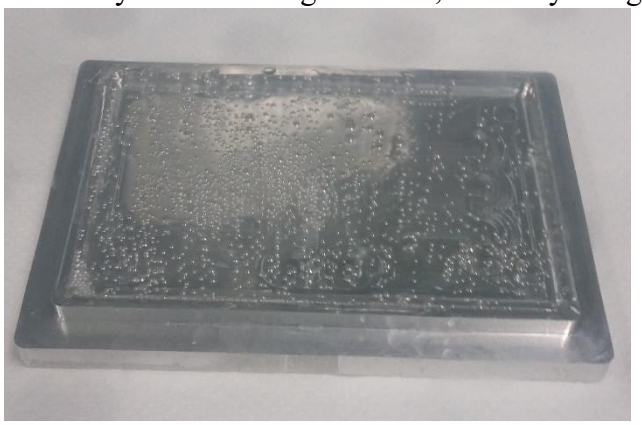

Figure 2.7 *Bubbles present inside the PDMS poured on the rigid master.*

10. Covering of the PDMS layer with scotch tape to protect the surface from dust contaminants and to preserve the surface characteristic before the following steps.

When necessary, the PDMS layer is properly cut to obtain the two single reactors; this operation is done right before plasma treatment and the cutting lines depend on the configuration chosen: reversible or irreversible.

2.1.6 Irreversible configuration

The irreversible configuration consists in the use of the plasma treatment to covalently bind the microfluidic platform and the supporting materials, usually a glass slide. Before proceeding with the plasma treatment, it is necessary to create the inlets for the fluid with a dispense tip (Nordson EFD) having an external diameter of 0.91 mm and the outlets and the seeding doors with a 1 mm diameter biopsy punch.

Then, the microfluidic platform is sealed irreversibly to a glass slide with the following procedure:

1. Cleaning of the device and of the glass base with scotch tape, to remove dust or any other residue from the surfaces;
2. Insertion of the two pieces, with the surfaces that must be activated facing upwards, inside the Plasma Cleaner (PDC-002-CE by Harrick Plasma, Figure 2.8a) and closing of the small door, keeping the valve closed (vertical position);
3. Switching on the vacuum pump to create vacuum inside the Plasma Cleaner;
4. After 5 minutes, the plasma is switched on at high power and, after its appearance, the valve is slightly opened (turning it counter clockwise) to allow the entrance of some air. The color of plasma should be an intense pink (Figure 2.8*b*), meaning that an adequate quantity of oxygen is present inside the chamber. If the color tends to violet or blue, it means that there is a lack of oxygen, and the valve should be gradually and

slightly opened (turning it clockwise). The plasma is maintained for 1 minute and 30

(a) *(b)*

Figure 2.8 *(a) Plasma Cleaner by Harrick Plasma used in BIAMET laboratory and (b) the colour of the plasma when the correct quantity of oxygen flows inside the chamber.*

seconds;

5. After 1 minute and 30 seconds, the plasma is switched off. Then the vacuum pump is switched off and the valve is slowly opened to return the chamber to atmospheric pressure.

Then the door is opened and the two layers are removed paying attention to not touching the activated surfaces. Afterwards, they are put into contact and they attach, thanks to the formation of chemical bonds, as explained in paragraph §1.2.3. To promote the total adhesion of all the surfaces it is possible to apply gentle pressure over the microfluidic platform, paying attention to avoid the collapse of the structures. Finally, the microfluidic platform is placed in the oven for 15 minutes at 65°C, to promote the formation of the covalent bonds.

The irreversible configuration can be used with soluble tracers (colored or fluorescent), to ensure the correct operations of the device, to validate the hydraulic seal of the all the doors punched and to qualitatively verify the formation of the chemical gradient inside the microchannels. In fact, since the whole platform is optically clear, all the channel and the central chamber can be observed visually as well as with the microscope.

The same configuration can be used to perform some biological validation of the platform, to investigate if cells can grow inside the central culture chamber. On the other hand, the irreversible configuration is not ideal for the final aim of these studies because of the difficulty in retrieving the sample of cells at the end of the experiments, and thus in performing specific post processing biological analysis.

2.1.7 Reversible configuration

A reversible configuration is designed to overcome the limitation imposed by the plasma treatment to create the hydraulic seal between the microfluidic platform and the support. This

configuration allows attaching the platform to the supporting material and its removal whenever necessary. The basic idea of this configuration is the use of a vacuum system to create a reversible adhesion between the micro-bioreactor and the glass slide. When the vacuum is active, the hydraulic seal between the platform and the support is ensured while, when the vacuum is released, the platform can be easily removed from its support.
The structure will be composed, from bottom to top, by the following:

- A glass slide 76x26 mm;
- A PDMS casing layer with a slab carved to accommodate a circular glass coverslip. This membrane is irreversibly attached to the glass slide.
- A PDMS vacuum layer with a circular cavity, the vacuum membrane, that allows the reversible sealing between the casing layer and the membrane itself. This membrane is irreversibly attached to the micro-bioreactor.

2.1.7.1 Photo lithography for the casing layer

In this section, the detailed protocol for photolithography fabrication of the mold for the casing layer will be described. The basic concepts of this technique are those described in §1.2.1.1
The procedure, that must be followed scrupulously, is:

1. **Design of the photomask**. The design of the photomask is done in AutoCAD®. Some rules of thumb to guarantee a perfect result are:
    - Scale unit in millimetres;
    - Length precision of *4 decimals*
    - Every closed figures must be formed by a single closed line
    - The final file extension must be a *.dwg format.*

    Than the file is imported in Adobe Illustrator® which allows to colour the photomask. The function of the photomask is to allow or prevent the passage UV light, so that in this case, since a negative photoresist will be used, the casing hole and the cutting lines are left transparent while the other surfaces are coloured in black. The detailed photomask and its dimensions is reported in Appendix in Section A.1.
2. **Pretreatement of silicon wafer**. The silicon wafer with a diameter of 76.2 mm is cleaned by sequential rinsing with Acetone (Sigma-Aldrich), Methanol (Sigma-Aldrich) and distilled water to ensure the perfect adhesion of the photoresist in the following steps. Then, the wafer is dried using compressed air and placed on a hot plate at 105°C for 10 minutes to completely remove humidity.

3. **Blanket layer: deposition of photoresist**. The function of the blanket layer is to promote the adhesion of the following layer. The silicon wafer is placed in a spin coater (WS-650-23NPP, Laurell, Figure 2.10) and it is secured to the chuck using vacuum generated by a pump (II-3-GD-T4 X, Edwards). Than a thin layer of SU-8 2005 photoresist (Microchem) is distributed and spin-coated over the wafer to obtain a thickness of about 5 microns. The desired thickness is achieved by selecting the proper spin protocol (Figure 2.9).

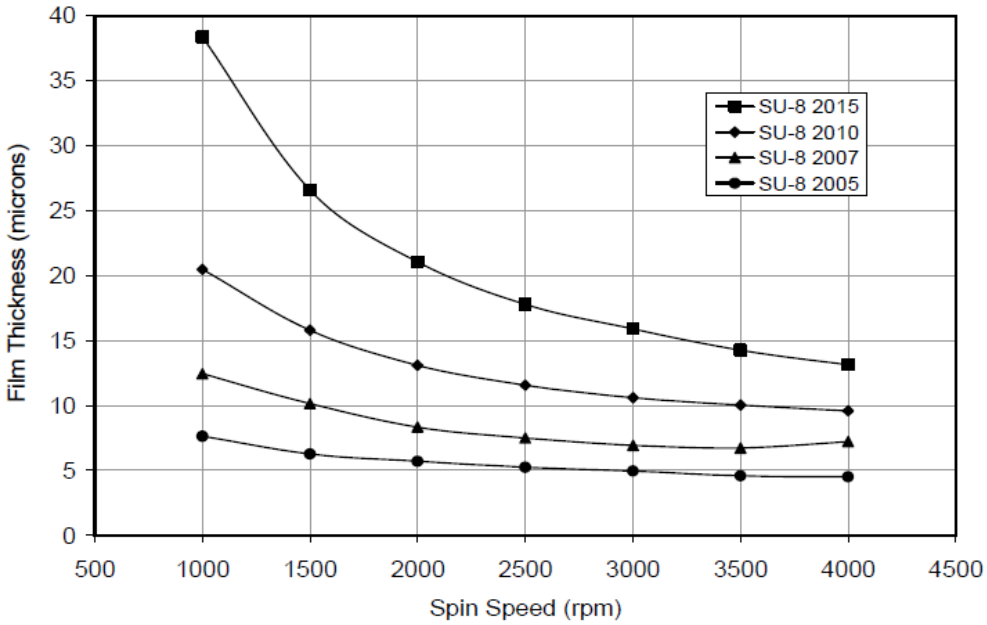

Figure 2.9 *Film thickness [μm] vs. spin speed [rpm] for the SU-8 2005, SU-8 2007, SU-8 2010 and SU-8 2015 photoresist; adapted from* [21].

The spin protocol in this case is:

- 1st step: 500 rpm for 10 seconds with an acceleration of 100 rpm/s;
- 2nd step: 3000 rpm for 35 seconds with an acceleration of 300 rpm/s.

The spinning step is carried out in an inert atmosphere, fluxing nitrogen inside the spin

Figure 2.10 *Spin coater (WS-650-23NPP, Laurell).*

coater. After spinning, the silicon wafer is left on a flat surface for ten minutes at room temperature to better homogenize the height of the photoresist.

4. **Blanket layer: soft bake and exposure**. Soft bake, a heating treatment of the photoresist, is used to remove the internal stresses of the material and to partially evaporate the solvent contained in the photoresist. Soft baking conditions depend on the height of the photoresist layer and they are reported in **Errore. L'origine riferimento non è stata trovata.**

Table 2.1 *Recommended soft bake times [min] in relation to the thickness [μm] of SU-8 2005 photoresist; adapted from* [21].

Thickness [μm]	Soft bake time at 95°C [min]
0.5-2	1
3-5	2
6-15	2-3
16-25	3-4

In this case the wafer is placed over a hot plate at 95°C for 2 minutes.

For the exposure step a UV lamp (Figure 2.11) with wavelength equal to 365 nm is used. The exposure energy E_{exp} in [mJ/cm^2] is set according to the height of photoresist desired as reported in Table 2.2.

Table 2.2 *Exposure energy [mJ/cm^2] vs thickness [μm] of SU-8 2005 Photoresist; adapted from* [21].

Thickness [μm]	Exposure energy [mJ/cm^2]
0.5-2	60-80
3-5	90-105
6-15	110-140
16-25	140-150

In this case the exposure energy is equal to 105 mJ/cm^2. Since the power P in [mW/cm^2] of the lamp is known, it is possible to calculate the exposure time in [s] using the following equation: [21]

$$t_{exp} = \frac{E_{exp}}{P} \tag{2.3}$$

At this step the wafer is placed under the UV lamp without the photomask to generate an smooth layer of photoresist over the entire surface of the silicon wafer.

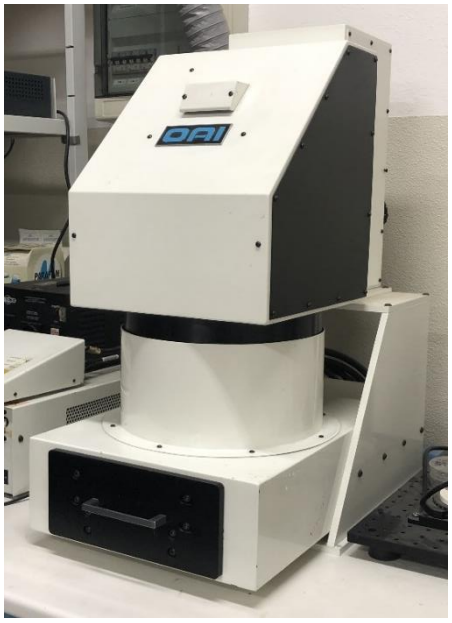

Figure 2.11 *UV lamp used to polymerize the photoresist.*

5. **Blanket layer: post exposure bake (PEB)**. It is now necessary another heat treatment to ensure the complete reticulation of the photoresist. Post exposure baking conditions depends on the thickness of the photoresist and, for the SU-8 2005 photoresist, they are reported in Table 2.3.

Table 2.3 *Recommended post exposure bake times [min] in relation to the thickness [µm] of SU-8 2005 photoresist; adapted from* [21].

Thickness [µm]	Post exposure bake time at 95°C [min]
0.5-2	1-2
3-5	2-3
6-15	3-4
16-25	4-5

In this case, the wafer is placed of the hot plat at 95°C for 3 minutes.

6. **Main layer: deposition of the photoresist**. The silicon wafer is placed in the spin coater and it is secured to the chuck. Nitrogen is fluxed to create an inert atmosphere. Than a layer of SU-8 2100 photoresist (Microchem) is distributed and spin-coated over the wafer to obtain a thickness of about 160 microns.
   The desired thickness of photoresist is achieved by selecting the proper spin protocol (Figure 2.12).
   The spin protocol in this case is:
   - 1st step: 500 rpm for 10 seconds with an acceleration of 100 rpm/s;
   - 2nd step: 2000 rpm for 35 seconds with an acceleration of 300 rpm/s.

After spinning, the silicon wafer is left on a flat surface for ten minutes at room temperature.

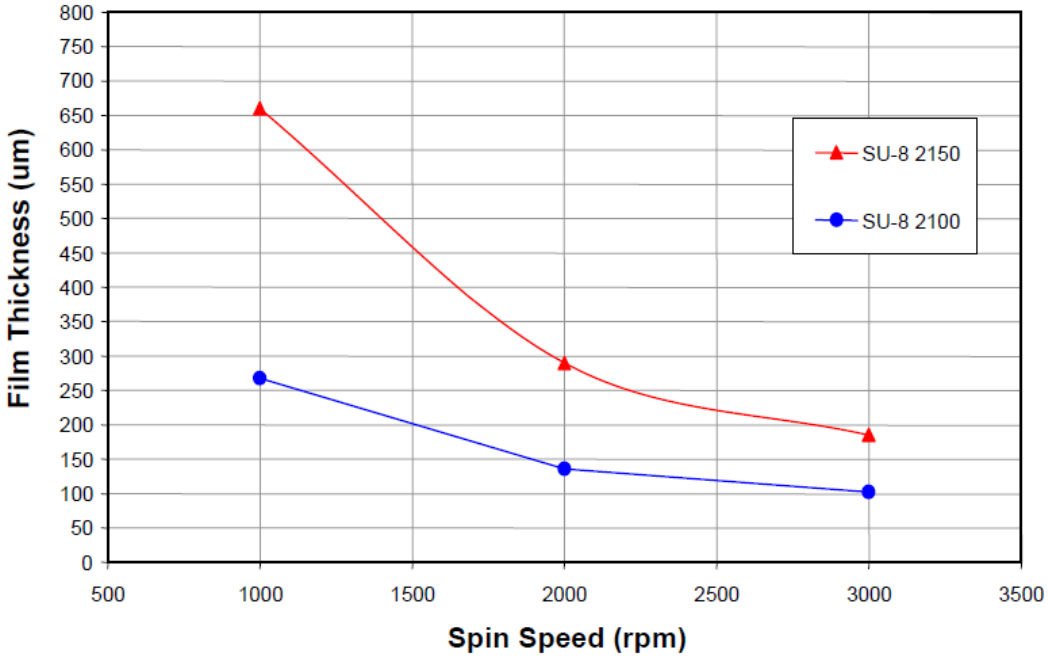

Figure 2.12 *Film thickness [µm] vs. spin speed [rpm] for the SU-8 2100 and SU-8 2150 photoresist; adapted from [23].*

7. **Main layer: soft bake and exposure**. Soft baking conditions depend on the height of the photoresist layer and they are reported in Table 2.4.

Table 2.4 *Recommended soft bake times [min] in relation to the thickness [µm] of SU-8 2100 photoresist; adapted from* [22].

Thickness [µm]	Soft bake time at 95°C [min]
100-150	20-30
160-225	30-45
230-270	45-60
280-550	60-120

In this case the wafer is placed over a hot plate at 95°C for 30 minutes.

For the exposure step a UV lamp with wavelength equal to 365 nm is used. The exposure energy E_{exp} in [mJ/cm^2] is set according to the height of photoresist desired as reported in Table 2.5.

Table 2.5 *Exposure energy [mJ/cm2] vs thickness [µm] of SU-8 2100 Photoresist; adapted from* [22].

Thickness [µm]	Exposure energy [mJ/cm^2]
100-150	240-260
160-225	260-350
230-270	350-370
280-550	370-600

In this case the exposure energy is equal to 260 mJ/cm^2. Since the power P in [mW/cm^2] of the lamp is known, it is possible to calculate the exposure time in [s] using equation 2.3

Then, the wafer is placed under the UV lamp. Before the exposure it is necessary to cover the wafer with the photomask, to selectively polymerize the negative photoresist in the areas exposed to UV light.

8. **Main layer: post exposure bake (PEB).** Post exposure baking conditions depends on the thickness of the photoresist and, for the SU-8 2100 photoresist, they are reported in Table 2.6.

Table 2.6 *Recommended post exposure bake times [min] in relation to the thickness [µm] of SU-8 2100 photoresist; adapted from* [22].

Thickness [µm]	Post exposure bake time at 95°C [min]
100-150	10-12
160-225	12-15
230-270	15-20
280-550	20-30

In this case, the wafer is placed over a hot plat at 95°C for 12 minutes.

The development step requires a solvent to dissolve the non-polymerized photoresist from the silicon wafer. A glass shallow beaker is placed over a rocking shaker and it is filled with Propylene monomethyl ether acetate (Sigma-Aldrich). The wafer is completely submerged into the solvent and the rocking shaker is switched on. The developing times depend on the thickness of the photoresist and they are reported in Table 2.7.

Table 2.7 *Recommended development times [min] in relation to the thickness [µm] of SU-8 2100 photoresist; adapted from* [22].

Thickness [µm]	Development time at 95°C [min]
100-150	10-15
160-225	15-17
230-270	17-20
280-550	20-30

In this case the development time is equal to 15 minutes

At the end of the development step, the wafer is rinsed thoroughly with Isopropyl alcohol (Sigma-Aldrich) and then dried with compressed air.

9. **Main layer: hard bake**. The last step of the photolithography technique is the hard bake, another thermal treatment. Hard bake can improve the mechanical and thermal characteristic of the master and ensure a good durability; it is carried out putting the wafer over a hot plate for 10 minutes at 65°C and then setting a ramp of 120°C/h for 2 hours to reach the maximum temperature of 160°C [22].

At the end of this step it is a good practice not to remove the wafer from the plate until it reaches room temperature to avoid any thermal shock of the material.

2.1.7.2 Photo lithography for the vacuum layer

In this section, the detailed protocol for photolithography fabrication of the mold for the casing layer will be described. The basic concepts of this technique are those described in §1.2.1.1

The procedure, that must be follow scrupulously, is:

1. **Design of the photomask.** The procedure is the same described in §2.1.7.2 at point one.
2. **Pretreatement of silicon wafer**. The procedure is the same described in §2.1.7.2 at point two.
3. **Blanket layer: deposition of photoresist**. The procedure is the same described in §2.1.7.2 at point three.
4. **Blanket layer: soft bake and exposure**. The procedure is the same described in §2.1.7.2 at point four.
5. **Blanket layer: post exposure bake (PEB).** The procedure is the same described in §2.1.7.2 at point five.
6. **Main layer: deposition of the photoresist.** The silicon wafer is insert in the spin coater and it is secured to the chuck. Nitrogen is fluxed to create an inert atmosphere. Than a layer of SU-8 2050 photoresist (Microchem) is distributed and spin-coated over the wafer to obtain a thickness of about 200 microns. The desired thickness of photoresist is achieved by selecting the proper spin protocol (Figure 2.12).

   The spin protocol in this case is:

   - 1st step: 500 rpm for 10 seconds with an acceleration of 100 rpm/s;
   - 2nd step: 1700 rpm for 30 seconds with an acceleration of 300 rpm/s.

   After spinning, the silicon wafer is left on a flat surface for ten minutes at room temperature.
7. **Main layer: soft bake and exposure.** Soft baking conditions depend on the height of the photoresist layer and they are reported in Table 2.4.

   In this case the wafer is placed over a hot plate at 95°C for 40 minutes.

   For the exposure step a UV lamp with wavelength equal to 365 nm is used. The exposure energy E_{exp} in [mJ/cm^2] is set according to the height of photoresist desired as reported in Table 2.5.

   In this case the exposure energy is equal to 320 mJ/cm^2. Since the power P in [mW/cm^2] of the lamp is known, it is possible to calculate the exposure time in [s] using equation 2.3

Then, the wafer is placed under the UV lamp. Before the exposure it is necessary to cover the wafer with the photomask, to polymerize the negative photoresist selectively in the areas exposed to UV light.

8. **Main layer: post exposure bake (PEB).** Post exposure baking conditions depends on the thickness of the photoresist and, for the SU-8 2100 photoresist, they are reported in Table 2.6.
   In this case, the wafer is placed of the hot plat at 95°C for 14 minutes. The development step requires a solvent to dissolve the non-polymerized photoresist from the silicon wafer. Similarly to what described above, the wafer is submerged into a Propylene monomethyl ether acetate (Sigma-Aldrich) bath inside a shallow beaker over a rocking shaker. The developing times depend on the thickness of the photoresist and they are reported in Table 2.7.
   In this case the development time is equal to 16 minutes
   At the end of the development step, the wafer is rinsed thoroughly with Isopropyl alcohol (Sigma-Aldrich) and then dried with compressed air.
9. **Main layer: hard bake**. Hard bake is carried out putting the wafer over a hot plate for 10 minutes at 65°C and then setting a ramp of 120°C/h for 2 hours to reach the maximum temperature of 160°C [22].
   At the end of this step it is a good practice not to remove the wafer from the plate until it reaches room temperature to avoid any thermal shock of the material.

2.1.7.3 Vacuum plant

It is necessary to develop a vacuum control system, in order to ensure the maintenance of the desired vacuum degree inside the vacuum ring. The vacuum plant will be formed by:

- A small vacuum pump;
- An electro valve;
- A digital vacuum switch;
- A surge tank;
- A vacuum pipe.

2.1.7.4 Replica molding in PDMS of the vacuum system

In this section the detailed protocol to produce the vacuum and the casing PDMS layers is described. The first step is the treatment of the silicon molds with Chlorotrimethylsilane (Sigma-Aldrich) vapor for 60 minutes to ease the separation of the polymerized PDMS layer from the mold.

The casing layer is prepared with the same procedure described in §2.1.5. In this case, 3 gr of PDMS are poured over the silicon wafer with the casing layer geometry in order to obtain a thin but easy to handle layer. At the end of the heating treatment step, the contour of the

casing layer is cut with a scalpel and peeled from the silicon wafer. Then, the PDMS casing layer is attached to the glass slide using plasma treatment, as described in §2.1.6.
The vacuum layer is produced by spin coating a layer of PDMS over the silicon mold to obtain a thickness of about 250 μm. PDMS is prepared as it is described in §2.1.5 in steps 1, 2 and 3. In this case, the spin protocol has one step at 300 rpm for 37 sec with an acceleration of 300 rpm/sec. The curing is performed on a hot plate with a heating ramp of 40°C/h for 2 hours, starting from room temperature and reaching the maximum temperature of 80°C. At the end of the heating step the vacuum configuration is assembled.
The main steps of the assembling procedure for the vacuum layer are the following:

1. The central chamber of the vacuum layer is cut with a scalpel and the layer surface is accurately cleaned with scotch tape;
2. The microfluidic platform is accurately prepared, creating the inlets of the fluid with a dispense tip (NORDON EDF) with external diameter of 0.91 mm, and the outlets and the seeding doors with a 1 mm diameter biopsy punch.
3. The PDMS and the silicon wafer with the PDMS layer are placed inside the plasma cleaner with the surfaces to be attached upwards;
4. The vacuum pump is switched on to create vacuum inside the plasma cleaner;
5. After 5 minutes, the plasma is switched on at high power and, after its appearance, the valve is slightly opened (turning it counter clockwise) to allow some air to enter the chamber. The color of plasma should be an intense pink, meaning that an adequate quantity of oxygen is present inside the chamber. The plasma is maintained for 2 minutes;
6. After 2 minutes, the plasma is switched off. Then the vacuum pump is switched off and the valve is slowly opened to return to atmospheric pressure.
7. The microfluidic platform and the silicon wafer are removed from the plasma cleaner and the microfluidic platform is positioned over the vacuum layer, following the alignment marks.
8. After the formation of the chemical bonds, the assembled parts are put in the oven for 15 minutes at 65°C;
9. Finally, the piece is cut following its sides, marked over the vacuum layer, and removed from the silicon wafer.
10. The last step is to punch the vacuum door with a dispense tip (NORDON EDF) with an external diameter of 0.91 mm.

Once both parts are prepared the micro-bioreactor can be assembled. A coverslip is put inside the casing hole and the vacuum layer, with the microfluidic platform attached, is positioned over it, using the alignment lines. The assembled device is then connected to the vacuum plant using a dispense tip (NORDON EDF) with an external diameter of 0.91 mm and a microtube (inner diameter of 0.5mm, outer diameter of 1.5mm, TYGON® TUBING). The

microtube is the connection between the dispense tip, inserted in the hole created in the microfluidic platform and in the vacuum layer, and the vacuum tube of the vacuum system.

2.1.8 Validation experiments

Both the irreversible and the reversible configurations are used to perform validation experiments, using colored (food coloring) and fluorescent tracers to verify if the desired fluid dynamic inside the platform is achieved.

The food coloring solution is prepared by mixing it with water, in a proportion suitable to obtain an intense color. This test gives a qualitative indication of the creation of the concentration gradient.

To obtain quantitative data it is necessary to perform validations using fluorescent tracers that can be visualized using a microscope. To do this, we used fluorescein isothiocyanate-dextrans (SIGMA-ALDRICH®). These are polymers of anhydroglucose, available in three different average molecular weights: 65000-85000, 250000 and 500000 Da. Their maximum excitation is at a wavelength of 490nm, and the maximum emission is at 520nm. The fluorescence increases with pH and is optimal at a value of 8 or above [23]. The average diffusion coefficient changes with respect to the molecular weight, and therefore, the three dextrans simulate solutes of different dimensions. The isothiocyanate-dextran solution is prepared by diluting it with milli-Q water in a proportion 0.0005g/10mL. The culture media is not used as a solvent for the fluorescent tracers, since it contains phenol red that can interfere with the fluorescence acquisitions and in this experiment no cells are present inside the reactor.

A syringe pump is used to infuse the solutions to the micro-bioreactor. The pump PHD Ultra (Harvard Apparatus) is supplied with a double mechanism that allows using pairs of syringes to simultaneously infuse and withdraw the fluids at the same flow rate.

The pump is formed by two elements: a central body with a display that allows to set up the pump, connected to a mechanical multi-rack remote unit, on which up to 10 syringes per side can be placed. The withdraw function is avoided to correctly simulate the fluid dynamic of the micro-bioreactor.

To carry out an experiment, two 10mL syringes (NYPRO) are prepared: two microtubes (inner diameter of 0.5mm, outer diameter of 1.5mm, TYGON® TUBING) are cut with the desired length and on one side a 21G steel dispensing tip (DRIFTON) is inserted inside and then connected to the syringe. On the other side of the tube a dispensing tip (DRIFTON), from which the plastic connector is removed, in inserted to facilitate the connection between the tube and the micro-bioreactor. One of the syringes is filled with the food coloring or with dextran solution and the other one is filled with milli-Q water, then they are placed on the infuse side of the pump. The type of syringe, the volumetric flow rates and the target volume are manually set on the display of the pump. The volumetric flow rates are usually set between 5 and 50 μL/min.

The procedure employed to validate the fluid dynamic of the micro-bioreactor and the hydraulic seal of the platform is now described in detail.

2.1.8.1 Irreversible configuration

The procedure followed to run the experiment is now reported:

- the micro-bioreactor is placed inside a petri dish and, using the syringe pump, the lateral channels, the micro-channels and the central chamber are completely filled with water (during this operation all the seeding doors and the inlets and outlets are left opened);
- the seeding doors are closed using a dispensing tip connected to a short piece of a closed microtube;
- the pump is started and once fluids have completely filled the tubing the inlets dispensing tip are insert in the inlet doors;
- after approximately 30 minutes the concentration gradient forms and reaches the steady state. It is not immediate, since the movement of the species inside the microchannels is led by diffusive flux.

Image of the gradient are taken at the beginning, after 10 and 30 minutes and 24 hours to verify the stability along the time of the steady state. During the experiments with food coloring, bright field pictures are enough to obtain a qualitative and semi-quantitative result, while during the experiments with dextrans, a fluorescence microscope is used to acquire data. The fluorescence microscope (Figure 2.13) used in BIAMET laboratory (Invitrogen EVOS^{TM} FL Cell Imaging System by ThermoFischer Scientific), is equipped of a monochrome camera, used for both transmitted light and fluorescence signals. The different EVOS Light Cubes installed (DAPI, GFP, RFP) allow using different fluorescence wavelengths. The GFP Cube is used with the fluorescent tracers. Using 10x and 4x

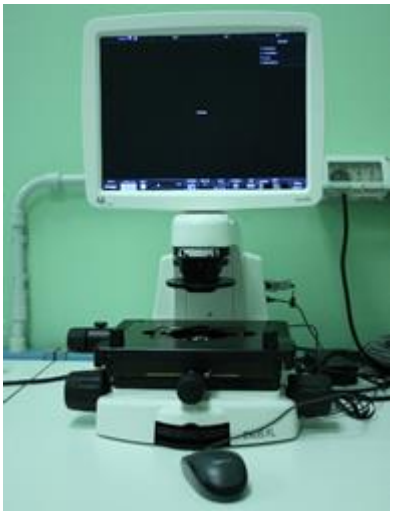

Figure 2.13 *Fluorescence microscope used in BIAMET laboratory.*

magnification, different images of series of micro-channels are taken and saved; afterwards, they are combined to obtain a picture of the entire section of the microfluidic platform.
The images are stitched with Paint®, and then the software ImageJ® is employed to obtain semi-quantitative information. The image is loaded, and then changed to an 8-bit type, to obtain a black and white picture. Using a square, 7 Regions of Interest (ROIs) are identified, and the medium light intensity is detected (commands Analyze and Measure). Since the absolute value of emission is not known, the twenty intensities are normalized with respect to the highest absolute value, to obtain a scale comparable with the results of the COMSOL Multhyphysics® simulation.

2.1.8.2 Hydraulic seal of the reversible configuration

To validate the hydraulic seal of the reversible configuration the microfluidic platform is assembled as described in §2.1.7.5. Then:

- The glass slide with the casing layer is placed inside a petri dish and a 15 mm diameter coverslip is inserted into the casing hole;
- The coverslip is covered with water using a micropipette and the vacuum layer with the micro-bioreactor is placed over it to assemble the reversible configuration; then the vacuum system is connected and the vacuum pump is switched on;
- Using the syringe pump, the lateral channels, the micro-channels and the central chamber are completely filled with water (during this operation all the seeding doors, the inlets and the outlets are left open);
- The seeding doors are closed using a dispensing tip connected to a short piece of a closed microtube;
- Two 10mL syringes (NYPRO) are prepared filling them with 10 mL of a solution of milli-Q water and food coloring (the presence of the color can visually indicate the success or failure of the hydraulic seal of the platform);
- The pump is started and once fluids have completely filled the tubing the inlets dispensing tip are insert in the inlet doors;
- After the colored fluid has completely filled all the micro-bioreactor, the flow rate is gradually increased of 10 μL/min each 30 minutes;

The hydraulic seal can be considered validated if there are no losses of fluid with a flow rate of 50 μL/min maintained for 6 hours.

2.2 Biological protocols and experiments

The cell line used during this work of thesis is HEK-293, provided by ATCC; they are human embryonic kidney cells, grown in tissue culture. Biologists widely used them in their researches because of their reliable growth and ease of transfection.

2.2.1 Cellular subculturing

The subculturing of cells is known as cellular splitting, and consists in the periodic separation of the cell population, in this case seeded in a $75cm^2$ flask. The aim is to avoid the overcrowding of cells that attach to the flask's bottom surface and to increase their number. A specific value of confluence (the filling percentage of the flask bottom surface) must not be exceeded, since cells would not be able to grow anymore. The HEK-293 cells have a maximum confluence of 90%. The culture media in which HEK-293 cells are bathed is prepared starting from the base medium, called DMEM (Dulbecco's Modified Eagle Media by Thermofisher Scientific). It does not contain any proteins, lipids or growth factors, so it is complemented to allow the supplying of nutrients and growth factors and assure the sterility of the cellular culture. The solution created, starting from 500 mL of DMEM, contains $10\%_{v/v}$ of fetal bovine serum (FBS), $1\%_{v/v}$ of Glutamine (an amino acid) and $1\%_{v/v}$ of Penstrep (an antibiotic). The mixture is filtered (with the Vacuum Driven Disposable Filtration System, Millipore) and stored at 4°C.

As far as the cellular splitting is concerned, this procedure is executed inside the biosafety cabinet (MSC-Advantage, Thermofisher Scientific), to ensure sterility and avoid any contamination of cells. First, culture media and Trypsin/EDTA solution (Biochrom GmbH) are warmed in a 37°C waterbath (Bagnomaria Serie Pura, Julabo, Sacco srl). Then, the old flask is taken from the incubator, placed in the biological hood, and the protocol is the following:

- The old medium (8 mL) is removed by aspiration with a serological pipet, and 4 mL are stored and kept in a 15 mL Falcon tube. The rest is discharged;
- The flask bottom surface is gently rinsed with 7 mL of sterile $PBS^{=}$ at room temperature, to remove any trace of culture media, that contains trypsin inhibitors. Then $PBS^{=}$ is aspirated and discarded;
- 1.5 mL of Trypsin (a serine protease used to cleave bonding proteins of cells to the dish) are added and it is distributed over all the cell layer; then the flask is placed in the incubator for 5 min. The detachment of cells can be observed by gently hitting the flask;
- The 4 mL of old medium are inserted in the flask, to inhibit the action of Trypsin. By gentle pipetting, the cells are aspirated from the bottom surface and placed in a 15 mL Falcon tube;
- At this point the cell suspension is diluted 1:10 µl with fresh medium: this cell suspension is used for counting, following the procedure described in §2.2.2;
- After counting, the cell suspension in the 15 mL Falcon tube is centrifuged at 950 rpm for 3 minutes, setting the soft deceleration mode. This procedure induces the

sedimentation of the cells that form a dense pellet, while the residues remain in the supernatant. The liquid is aspired and the cells are suspended in the desired quantity of new culture media;

- Finally an appropriate aliquot of cell suspension is added to a new 75 cm^2 flask, with 8 mL of fresh culture media. An inoculum of $2 \cdot 10^3$ to $6 \cdot 10^3$ cells/cm^2 is recommended.

The cellular splitting is usually done every 3-4 days. However, the medium renewal may be necessary every 2-3 days. The medium must be replaced when its color changes from red to yellow. It means that its pH has changed, because of the depletion of nutrients and growth factors and accumulation of waste products by the cells.

2.2.2 Cellular counting

The cellular counting procedure is necessary whenever the number of cells must be known, for example during splitting or during the seeding of the microbioreactors in the biological experiments. To carry out this counting procedure the Bürker chamber (Figure 2.14) is employed: it is formed by a rectangular microscope slide with a rectangular indentation that creates a chamber. The chamber is engraved with a laser-etched grid of perpendicular lines.

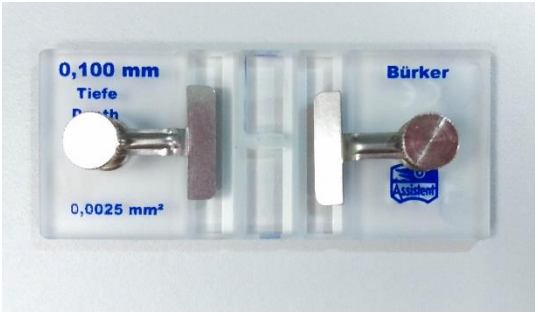

Figure 2.14 *Bürker chamber.*

The area enclosed by the lines is known, as well as the volume of the chamber. Therefore, it is possible to count the number of cells present in a specific volume of fluid, and so the total number of cells.

The Bürker chamber has two 3 x 3 mm cells, with a depth of 0.1mm. Each cell is divided in 9 squares (1 mm side), each one divided in 16 squares (0.2 mm side).

The chamber is prepared by placing a squared glass slide of the proper dimensions over the chamber and fixing it with two lateral latches; then this protocol is followed:

- The cell suspension is diluted 1:10 with some fresh culture media and pipetted in order to avoid sedimentation and clustering of cells.
- 10 µL of this new cell suspension are collected with a micropipette and positioned on one side of the Bürker chamber, forming a bubble. Then 10 µL of Trypan Blue (Invitrogen), a cell stain that colors only dead cells, are mixed with the cells by

pipetting. Viable cells do not take up this dye, since their membrane is impermeable, but dead cells' membrane is permeable and so they become blue.

- 10 µL of the mixture (cell suspension in Trypan Blue) are injected between the chamber and the glass slide by capillarity.
- The chamber is observed at the microscope with a 10x enlargement. At least 3 random squares (1 mm side) are considered: the number of live cells is counted for each square, considering only the cells that are completely inside the medium border line of the 1 mm side square, then the arithmetic mean is calculated. In Figure 2.13 it is highlighted the difference between live cells (in green), dead cells (in red) and residues (in blue) in a square.

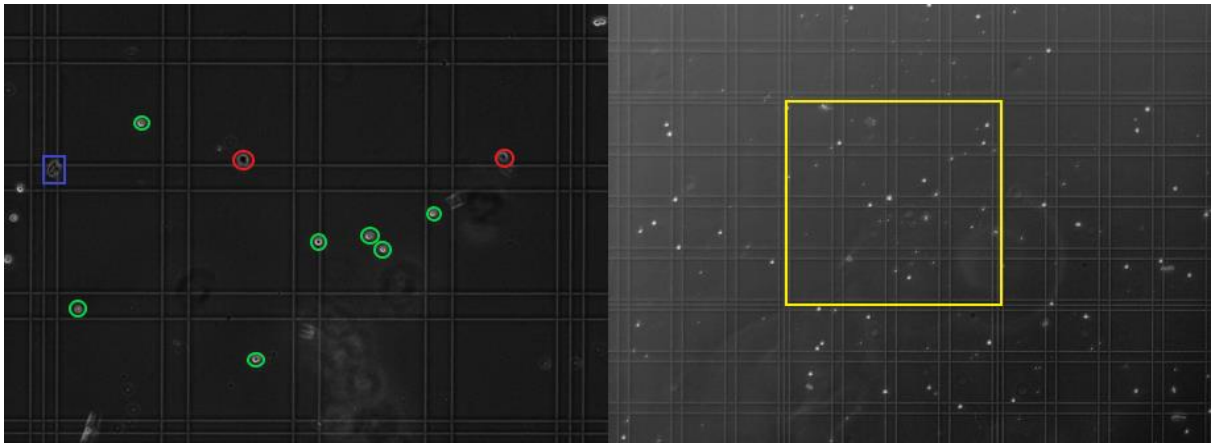

Figure 2.15 *One square of the Bürker chamber: on the left, the green circles highlight live cells, the red circles highlight dead cells and the blue square is positioned on one residue.*

Finally, knowing the mean number of cells per square (N_{mean}), the concentration of cells can be calculated as follows:

$$N\left(\frac{cells}{mL}\right) = N_{mean}\left(\frac{cells}{square}\right) \cdot 2 \cdot 10 \cdot 10000 \qquad (2.4)$$

where 2 and 10 are the dilution factors (respectively 2 for the dilution with Trypan Blue and 10 for the dilution with fresh culture media) and 10000 is a coefficient used in this calculation, that includes information about the geometry and the volume of the chamber. The number of cells per mL is obtained, and this value can be multiplied for the total volume to obtain the total number of cells.

2.1.9 Biological validation experiments

Some biological tests are performed in order to assess the biological compatibility of the µ-bioreactor. For the biological experiments, all the materials needed must be sterilized with

vapor at 121 °C in the autoclave (Europa B Evo, Arco Scientifica), and all the operations of the procedure are conducted inside a biological safety cabinet.

The first step is to place the µBR inside a Petri dish under the biosafety cabinet. Then, before seeding cells it is necessary to coat the µBR surface to promote adhesion of cells to the glass slide. In this case 10 µL of fibronectin solution (FN, a protein that favors the attachment of cells to the PDMS surface), diluted with $PBS^{=}$ in a proportion 1:4, are carefully injected in the central chamber from a seeding port, using a micropipette. After 1h, the same volume of cells, at the desired density in their culture media, is seeded in the central chamber.

After a few hours, the cells start adhering to the bottom surface. At this point, 200-300 µL of culture media are placed over all the holes of the platform, to ensure availability of nutrients and ideal survival environment for the cells during static culture. The platform is left overnight (or for a maximum of two days) in the incubator. Before starting the experiments, the two seeding ports are plugged using two dispensing tips connected to a short piece of a closed microtube.

The biological experiments consists in staining cells using fluorescent substances that have specific affinity to one substrate, so they mark one specific target selectively; in this case the fluorescent tracers that highlight the presence of cells are:

- Hoechst (trihydrochloride, triydrate), a blue fluorescent dye used to stain DNA, excited by UV light at 350 nm and with a maximum emission at 461nm. The Hoechst supplied by Thermo Fisher Scientific (10 mg) is used to prepare a 16.23 mM (10 mg/mL) stock solution, by diluting it in 10 mL of deionized water. The 10 mg/mL Hoechst stock solution may be stored at 2–6°C for up to 6 months or at –20°C for longer periods. To prepare the Hoechst staining solution, the stock solution must be diluted 1:2000 in DMEM [24];
- Calcein-AM (SIGMA-ALDRICH), a reagent staining the cytoplasm in cells, with a maximum excitement at 496nm and emission at 516nm. The Calcein-AM supplied by the producer (1mg, that corresponds to 1µmol) is used to prepare a 10mM stock solution, by diluting it in 100µL of dimethyl sulfoxide (DMSO) and stored at -20 °C. In order to obtain a 10µM working solution, 10µL of stock solution must be diluted in 10mL of culture media.

The syringes are prepared, one filled with DAPI and one with Calcein-AM paying attention to cover both with aluminum foil (the two fluorescent tracers are light sensitive). The pump is started and once fluids have completely filled the tubing, the inlets dispensing tip are inserted in the inlet doors of the micro-bioreactors. After two hours, necessary to allow the tracers to enter the cells, images are taken with the microscope, using the DAPI Cube for the DAPI dye and the GFP Cube for the Calcein-AM. Therefore, the concentration gradient can be verified in both the directions, and the cell viability is observed.

Chapter 3

Results and discussion

This Chapter reports the design of the micro-bioreactor, the fluid dynamic simulations carried out to obtain the final microbioreactor configuration and the final shape of the platform. Then the results of the validation experiments are reported. Finally it is tested the biological compatibility of the microfluidic platform.

3.1 Gradient generators

3.1.1 Design of the micro-bioreactor

The actual design is a modification of a micro-bioreactor developed in a previous work of thesis. The platform (Figure 3.1) is composed by:

- two lateral channels used to flow the two fluids at different concentrations;
- two series of microchannels that connect the lateral channels and the central chamber;
- a central culture chamber, where the cells are seeded, equipped of two seeding doors, useful to inject the cells inside the micro-bioreactor.

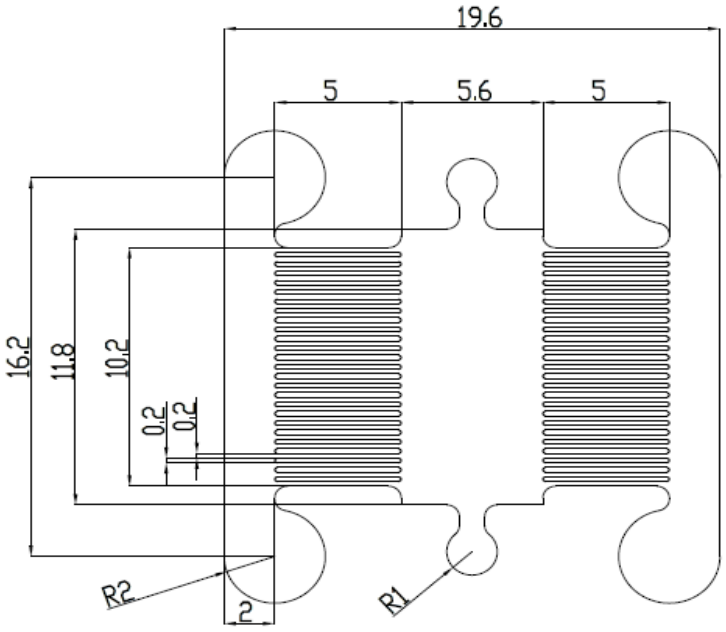

Figure 3.1 *Design of the micro-bioreactor developed in a previous work of thesis..*

The main dimensions of the micro-bioreactor in Figure 3.1 are reported in Table 3.1.

Table 3.1 *Main dimensions of the micro-bioreactor.*

Dimensions		Values
Width of the lateral channels	[mm]	2.00
Height of the lateral channels	[mm]	0.12
Width of the micro-channels	[mm]	0.20
Height of the micro-channels	[mm]	0.12
Length of the micro-channels	[mm]	5.00
Width of the central chamber	[mm]	5.60
Height of the central chamber	[mm]	0.12
Length of the central chamber	[mm]	11.80
Surface of the central chamber	[mm^2]	66.08
Volume of the central chamber	[mm^3]	7.92

The two fluids that feed the device enter from one side of the lateral channels and are removed from the other side at constant flow rate, ensuring maintenance of the steady state condition. It is also fundamental to achieve laminar conditions inside the entire device, including in the lateral channels. To exemplify the procedure to validate the establishment of a laminar profile, we evaluate the Re number inside the lateral channels; they have rectangular section (120 x 2000µm) and we considered a typical inlet flow rate of 5µL/min ($8.33 \cdot 10^{-11}$ m^3/s). To evaluate Re (3.2) it is necessary to calculate the equivalent diameter (3.1), taking into consideration the parameters reported in Table 1.2:

$$D_{eq} = \frac{4S}{2P} = 2.26 \cdot 10^{-4} m \tag{3.1}$$

$$Re = \frac{\rho v D_{eq}}{\mu} = 7.8 \cdot 10^{-2} \tag{3.2}$$

From the calculation, we can conclude that flow inside the lateral channels is clearly laminar, since Re is less than one.

The general objective of the use of this platform is to obtain a shear-free concentration gradient inside the central chamber. This means that inside the chamber the diffusive flux must dominate over the convective one. This is not possible using the old configuration so a new µ-bioreactor is studied.

The convective transport component inside the microchannels must be reduced, thus, it is needed to understand which parameters must be considered and eventually modified to change the Péclet number. Its value, that expresses the ratio between the convective flux and the diffusive one, depends on: the velocity of fluid inside the micro channel, the equivalent diameter of the micro channel and the diffusion coefficient of the species *i*, that

is constant for each species if the temperature is constant. Therefore, the main parameters that should be studied are:

- the aspect ratio (length/height of the channel)
- the geometry of the microchannels (shape and dimensions)

The velocity inside the micro channels cannot be considered a parameter because its punctual value depends on both parameters listed above. Thus, a combined study is done to obtain the final design.

Before proceeding, it is important to consider some limitation of the master's production technique: the minimum width of the microchannels is 150µm, and the height can vary in a range between 10 and 450 µm. These limitations are imposed by the dimensions of the tools of the micromiller and by their wear during the milling of the Aluminum block.

The first step consists in the investigation of how the Péclet number varies within a variation of the aspect ratio, without changing the rectangular shape of the micro-channels. To carry out this analysis two of the three dimensions are fixed, while the height is varied. In Table 3.2 are listed the values used in this sensitivity analysis.

Table 3.2 *Dimensions and values used in the Péclet number sensitivity analysis*

Dimensions		Values
Width of the micro-channels	[µm]	150
Length of the micro-channels	[µm]	5000
Height of the micro-channels	[µm]	10-150

Since the height of the other elements of the platform is kept constant (120µm), this is the maximum height of the micro-channels. These calculations are carried out assuming that the velocity is constant and fixed at a value of 10^{-6} m/s, which is an approximation, since the velocity itself depends on the height of the micro-channels. The value set for the velocity represent only the order of magnitude of the velocity profile inside the micro-channels in the old micro-bioreactor. The trend of Pe is shown in Figure 3.2. It can be seen how Péclet values reduce as the height of the micro-channels is reduced.

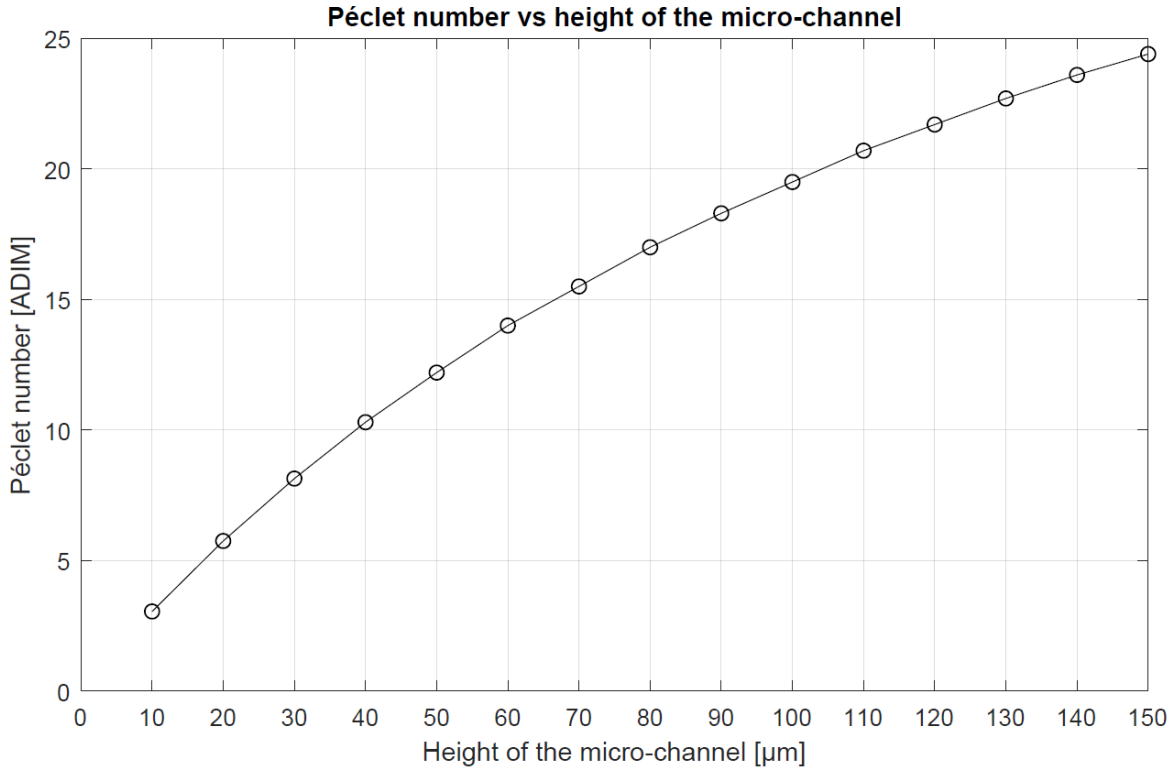

Figure 3.2 *Variation of Pèclet number varying the height of the micro-channels*

Even if this is only a first calculation to understand the trend of this important parameter, it is clear how the height of the micro-channels should be small than possible but not under 10 µm.

A further study is done to evaluate if it is useful to modify the geometry of the micro-channels. The purpose is to increase the pressure loss along the micro-channels in order to reduce the velocity of the fluid inside the central chamber. Two different geometry are analyzed and compared; the first one, represented in Figure 3.3, involves the adding of

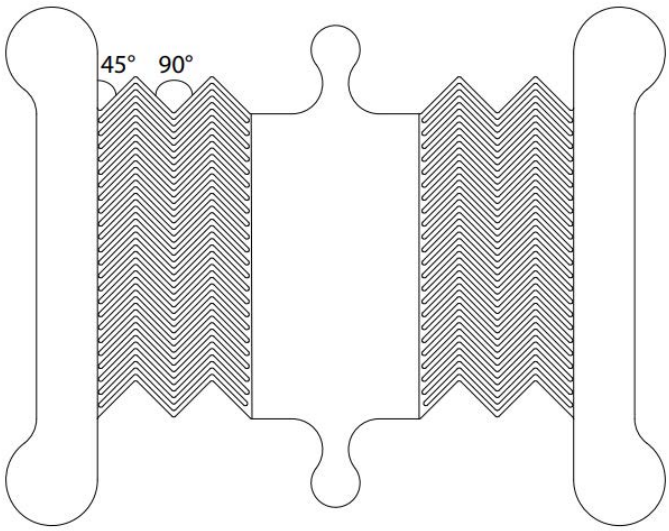

Figure 3.3 *Micro-bioreactor with non-linear micro-channels. Three 90° radius elbow and two 45° radius elbow are added.*

three 90° radius elbow and two 45° radius elbow. As can be seen from Figure 3.3 the geometry of the inlets and outlets is changed in order to facilitate the micro-milling procedure. In this case, the length of each micro-channel is increased and the tortuosity generated by the adding of the elbows could increase the pressure loss.
The main dimensions of the considered configuration and the pressure loss calculated along a micro-channel are reported in Table 3.3.

Table 3.3 *Main dimensions of the non-linear micro-channels configuration and the pressure loss calculated along a micro-channel.*

Dimensions	Values	Unit of measure
Width of the lateral channels	2.00	[mm]
Height of the lateral channels	0.12	[mm]
Width of the micro-channels	0.15	[mm]
Height of the micro-channels	0.01	[mm]
Distance between the lateral channel and the central chamber	5.00	[mm]
Equivalent length of the micro-channels	8.40	[mm]
Width of the central chamber	5.60	[mm]
Height of the central chamber	0.12	[mm]
Length of the central chamber	10.00	[mm]
Surface of the central chamber	56.00	[mm^2]
Volume of the central chamber	6.72	[mm^3]
Pressure loss along each micro-channel	$7.65*10^{-2}$	[Pa]

As it can be seen the width and the height of the micro-channels are reduced to their minimum value allowed. The pressure loss are calculated assuming a velocity of 10^{-7} m/s

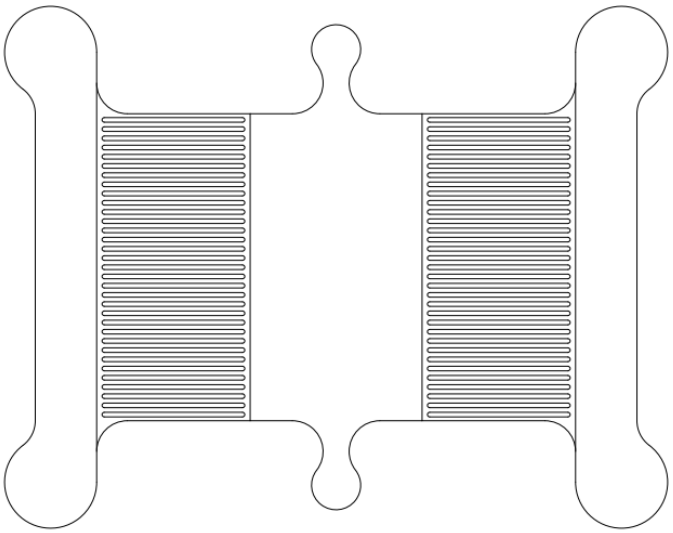

Figure 3.4 *Micro-bioreactor with linear micro-channels.*

inside each micro-channel and using the equivalent length method, which will be described in Appendix A.2.

In the second geometry analyzed, the micro-channels shape is maintained constant with respect to the micro-bioreactor developed in the previous work of thesis, but their dimensions are changed. The width and the height of the micro-channels are reduced to their minimum value allowed. Figure 3.4 shows the second geometry analyzed.

The pressure losses calculated and the main dimensions of the considered geometry are reported in Table 3.4.

Table 3.4 *Main dimensions of the linear micro-channels configuration and the pressure loss calculated along a micro-channel.*

Dimensions	Values	Unit of measure
Width of the lateral channels	2.00	[mm]
Height of the lateral channels	0.12	[mm]
Width of the micro-channels	0.15	[mm]
Height of the micro-channels	0.01	[mm]
Length of the micro-channels	5.00	[mm]
Width of the central chamber	5.60	[mm]
Height of the central chamber	0.12	[mm]
Length of the central chamber	10.00	[mm]
Surface of the central chamber	56.00	[mm^2]
Volume of the central chamber	6.72	[mm^3]
Pressure loss along each micro-channel	$4.55*10^{-2}$	[Pa]

As in the first case, pressure losses are calculated assuming a velocity of 10^{-7} m/s inside each micro-channel.

Comparing the two configurations, it is clear that the pressure losses increase within the tortuosity of the micro-channels, but they remains on the same order of magnitude in both geometries. On the other hand, as far as the master production procedure is concerned, it is clear that the geometry described in Figure 3.3 increases a lot the complexity of the micro-milling processes. In addition, increasing the complexity of the micro-milling procedure, will lower the grade of precision of the structure milled. For this reasons, the second configurations (reported in Figure 3.4) is the most suitable and the once that it is developed in this work of thesis.

3.1.2 COMSOL Multiphysics® simulations

The COMSOL Multiphysics® simulation is used to understand the mode of operation of the device

In 2D and 3D simulations the lateral channels are drawn as rectangles or parallelepipeds, respectively, and the seeding ports are not added to the geometry since they do not contribute to the fluid dynamics of the device.
In all 3D simulations, a normal mesh is built and a study is conducted. In 2D simulations, thanks to the simplified geometry, a mesh with finer elements size is built.

3.1.2.1 Laminar flow

The laminar flow is set on the entire platform to solve the Navier-Stokes equations for the single-phase fluid at the steady state. In this case a 3D simulation is carried out. The fluid is assumed to enter the two upper sides of the lateral channels, while it exits via the two lower sides. Knowing the inlet flow rates typically set during the experiments, the inlet average velocity is calculated dividing them for the section of the channel ($2.4 \cdot 10^{-7}$ m^2). In Table 3.5 are reported the flow rates, and the corresponding average velocities, employed in the simulations.

Table 3.5 *Values of flow rates and corresponding average velocities used in the COMSOL simulation of the microfluidic platform.*

Case	Flow rate [µL/min]	Flow rate [m^3/s]	Velocity [m/s]
1	5	$8.33 \cdot 10^{-11}$	$3.47 \cdot 10^{-4}$
2	10	$1.67 \cdot 10^{-10}$	$6.96 \cdot 10^{-4}$
3	15	$2.5 \cdot 10^{-10}$	$1.04 \cdot 10^{-3}$

In correspondence to the outlets of the fluids, the relative pressure is set as equal to zero. The temperature is 293.15K.
The surface velocity profile at the middle section of the central chamber for case 1 is shown in Figure 3.5. As it can be seen the solution is not perfectly stable; this suggests that a finer mesh is needed.

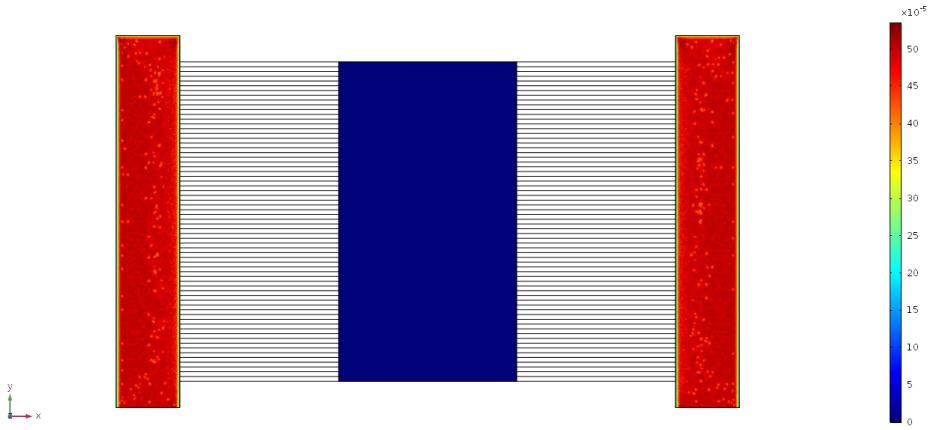

Figure 3.5 *Surface velocity profile at the middle section of the central chamber for case 1.*

The velocity inside the central chamber is very small and can vary between zero and $2*10^{-8}$ m/s. The laminar regime is ensured since the calculated Reynolds number is always below

10^{-3}. Figure 3 6 shows the Reynolds number profile at the middle section of the central chamber for case 1.

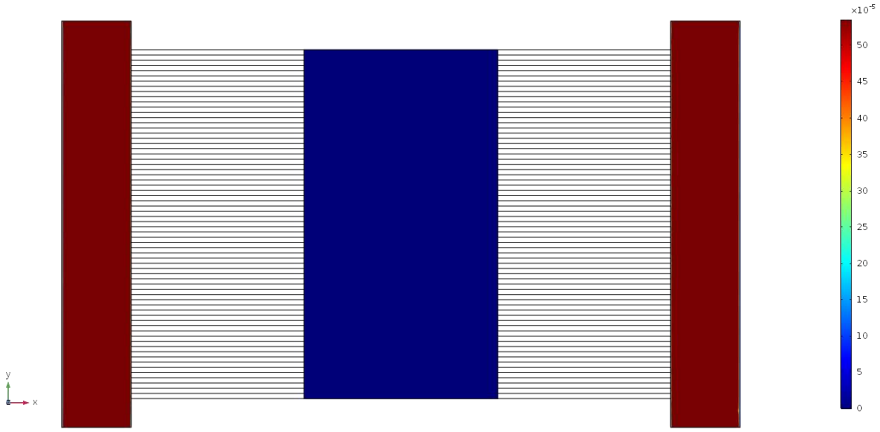

Figure 3 6 *Reynolds number profile at the middle section of the central chamber for case 1.*

The same results are obtained for cases 2 and 3.

3.2.2.2 Transport of Diluted Species

The addition of the Transport of Diluted Species interface, as explained in paragraph §2.1.2.2, does not require the properties of the species *i*, except for the diffusion coefficient. The species that are taken into consideration are the exosomes and the three fluorescent tracers available. The diffusion coefficient of exosomes in water is calculated with the Stokes-Einstein equation (equation 1.13), and considering an average diameter of exosomes of 70nm ($7 \cdot 10^{-8}$ m). Its value is $3.14*10^{-12}$ m^2/s.

In order to calculate the diffusion coefficient of the three fluorescent tracers in water, it is necessary to calculate their radius. The producer of dextrans, SIGMA-ALDRICH, provides information about the trend of the average Stokes radius of the particles (considered as spherical) with respect to the molecular weight, as reported in Table 3.6.

Table 3.6 *Stokes radius of the fluorescent isothiocyanate dextran with respect to the molecular weight [23].*

Molecular weight [Da]	Stokes radius [Å]
4000	14
10000	23
20000	33
40000	45
70000	60
150000	85

Starting from these data, a regression curve of the Stokes radii with respect to the molecular weight has been calculated. The result of the regression is reported in Figure 3.7.

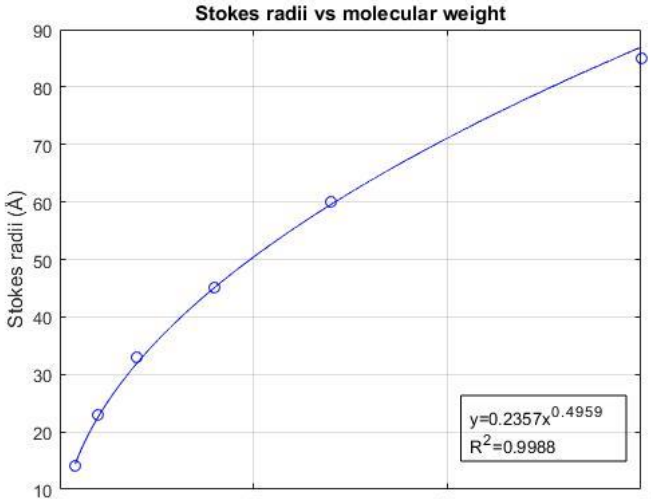

Figure 3.7 *Regression curve of the Stokes radii of the isothiocyanate-dextrans with respect to the molecular weight.*

The three radii can be extrapolated from the curve and the diffusion coefficient can be calculated with the Stokes-Einstein equation. All the values calculated are reported in Table 3.7.

Table 3.7 *Stokes radii and diffusion coefficients of the three fluorescent isothiocyanate-dextrans available, calculated starting from the regression curve.*

Molecular weight [kDa]	Stokes radius [Å]	Diffusion coeff. in water [m^2/s]
75	62	$3.48 \cdot 10^{-11}$
250	112	$1.92 \cdot 10^{-11}$
500	158	$1.36 \cdot 10^{-11}$

It can be observed that the three fluorescent isothiocyanate dextrans have diffusion coefficients with the same order of magnitude. Therefore, it is expected to have similar results from the simulations. The exosomes' diffusion coefficient is one order of magnitude smaller with respect to the tracers' one, because of the bigger dimensions.

The second information needed is the initial concentration c of the species at the inlets. At one inlet (usually the left-hand one) the concentration is set at an arbitrary value, while at the other one the concentration is set as equal to zero. The final graphs are created by normalizing the concentration, dividing it for the initial value, to obtain a dimensionless scale (from zero to one), easily comparable with the quantitative results of the experimental validations.

The convergence of this simulation is not easy. Adding the Transport of Diluted Species interface makes impossible to find a solution in the 3D domain. The geometry of the system does not allow initializing the solution in a coarser domain, so once a fine domain

is set, the software is not able to converge. To avoid this limitation and to obtain a trend of the concentration gradient inside the µ-bioreactor a 2D simulation is performed. The main limitation of this type of study is that the 2D simulation does not take into account of the different height of the structures. The wall effect of the small geometry of the micro-channels is not considered at all.

To obtain a quite reasonable result, the 2D simulation is initialize using values of velocity obtained from the 3D velocity field simulation. In the detail the inlet velocity of the lateral chamber is set equal to 10^{-6} m/s, which is the mean value at the inlet of the micro-channels in the 3D simulation for case 1.

The concentration profile obtain seems reasonable, looking at the small values of the velocity inside the central chamber. Figure 3.8 shows the qualitative expected concentration profile.

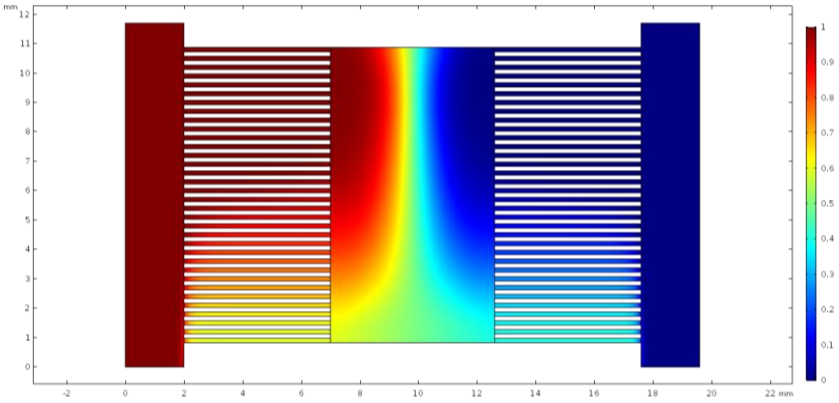

Figure 3.8 *Concentration gradient inside the central chamber obtained using a 2D simulation.*

From this simulation it is possible to obtain the concentration values inside the central chamber; these values are compared with the data obtained from the platform validation experiment.

3.1.2 Production of the master

As explained in paragraph §2.1.3, the master of the microfluidic platform is produced with a micromiller. The detailed project of the mold is reported in Figure 3.10. It can be noticed the presence of the alignment marks, added to easily align the vacuum layer to the µ-bioreactor.

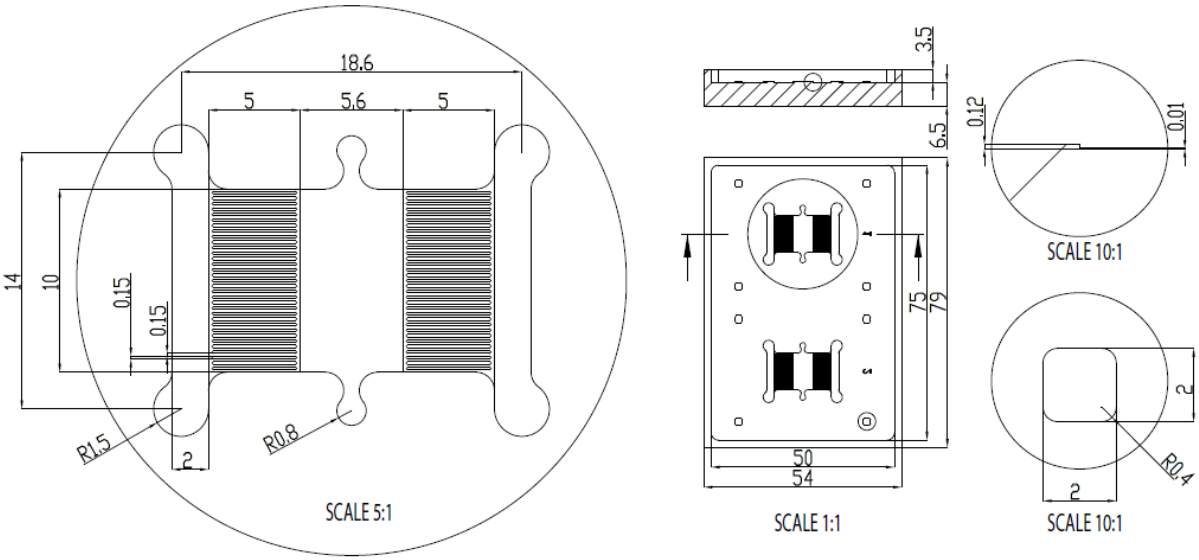

Figure 3.10 *Design of the master of the µ-bioreactor.*

Figure 3.9 shows the final aluminium master obtained at the end of the micromilling process.

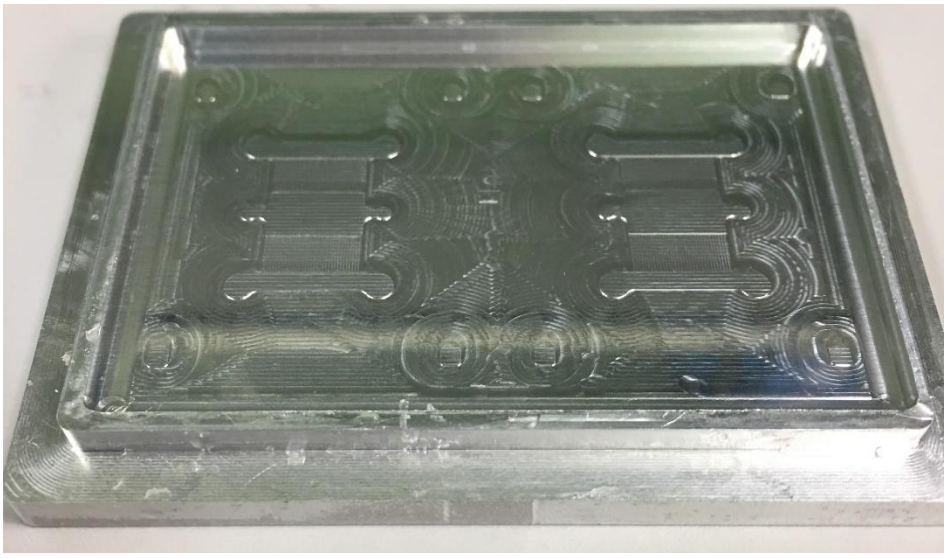

Figure 3.9 *Aluminium master of the µ-bioreactor.*

Some tests are performed to understand the quality of the master produced. The 3D optical profiler can provide information about the heights of the master.

The heights of specific areas of interest are studied with the Focus Variation mode. The areas are identified in Figure 3.12.

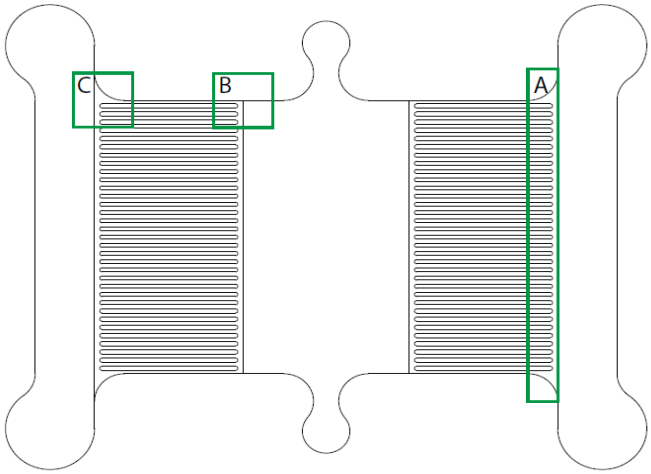

Figure 3.12 *Area of interest used to carry out the profilometric analysis.*

Area A it is useful to analyze the relative height between the micro-channels. The results are reported in Figure 3.11.

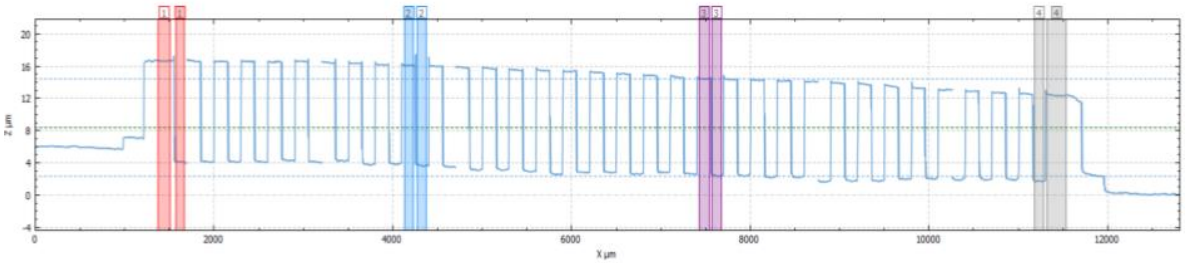

Figure 3.11 *Profilometric plot of area A.*

The four areas highlighted correspond to four channels and are used to understand if the measures of the master correspond to those of the project.

Table 3.8 reports the results. It can be seen that the micro-channels heights are not homogenous but, since the difference is on the order of 1-2 microns, this variation can be neglected. This fact is confirmed looking at the pressure loses along a micro-channel varying its height between 8 and 12 µm. It can be seen in Table 3.9 that the order of magnitude is the same for all the heights.

Table 3.8 *Results of the profilometric analysis for area A.*

Measure region	Value [µm]
Design	10.00
Region 1	12.50
Region 2	12.40
Region 3	12.01
Region 4	10.63

Table 3.9 *Pressure drops along the micro-channels calculated varying the height of the micro-channels.*

Height of the micro-channel [µm]	Pressure drops [Pa]
8	$2.25*10^{-2}$
9	$2.26*10^{-2}$
10	$2.28*10^{-2}$
11	$2.29*10^{-2}$
12	$2.30*10^{-2}$

In area B the relative height between the central chamber, the outer region and the micro-channels are analyzed. The profilometric plot of the measure of the relative height between the central chamber and the outer region is reported in Figure 3.13.

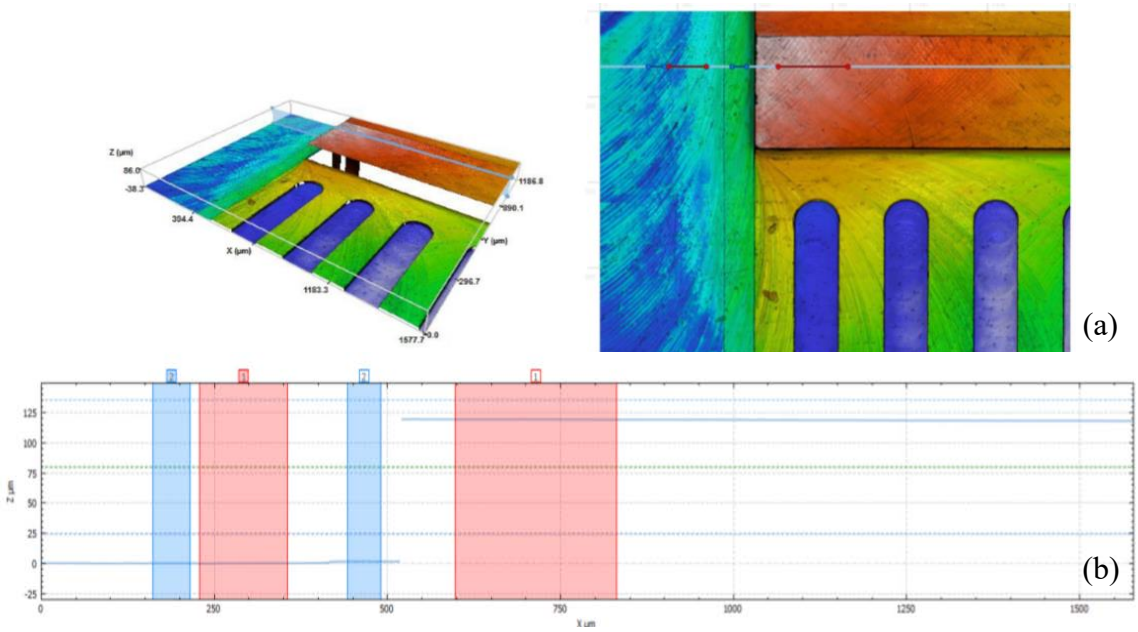

Figure 3.13 *(a) 3D view of the interest area. (b) Results of the profilometric analysis to quantify the relative height between the central chamber and the outer region.*

The profilometric plot of the measure of the relative height between the central chamber and the micro-channel is reported in Figure 3.14.

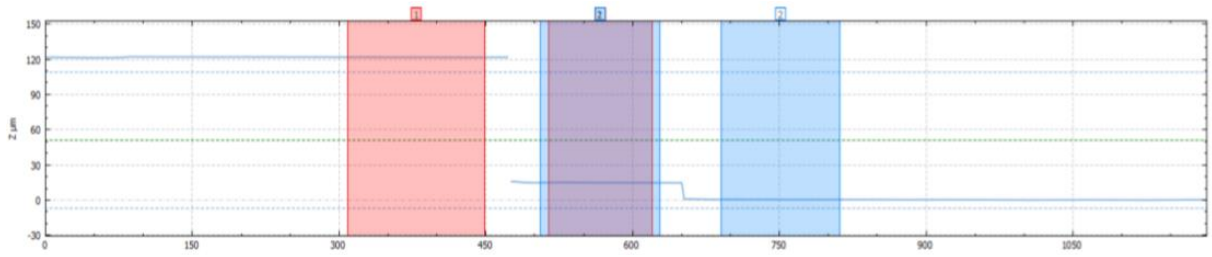

Figure 3.14 *Results of the profilometric analysis to quantify the relative height between the central chamber and the micro-channel.*

Table 3.10 shows the results for area B. Also in this case, even if the measures do not perfectly correspond to the design ones, these differences are so small that can be neglected.

Table 3.10 *Results of the profilometric anaysis for area B.*

Measure region	Design value [µm]	Measured value [µm]
Height of the micro-channel	10.00	14.32
Central chamber vs outer region	120.00	119.25
Central chamber vs micro-channel	110	106.77

In area C the relative height between the lateral channel, the outer region and the micro-channels are analyzed. The profilometric plot of the measure of the relative height between the lateral channel and the outer region is reported in Figure 3.15.

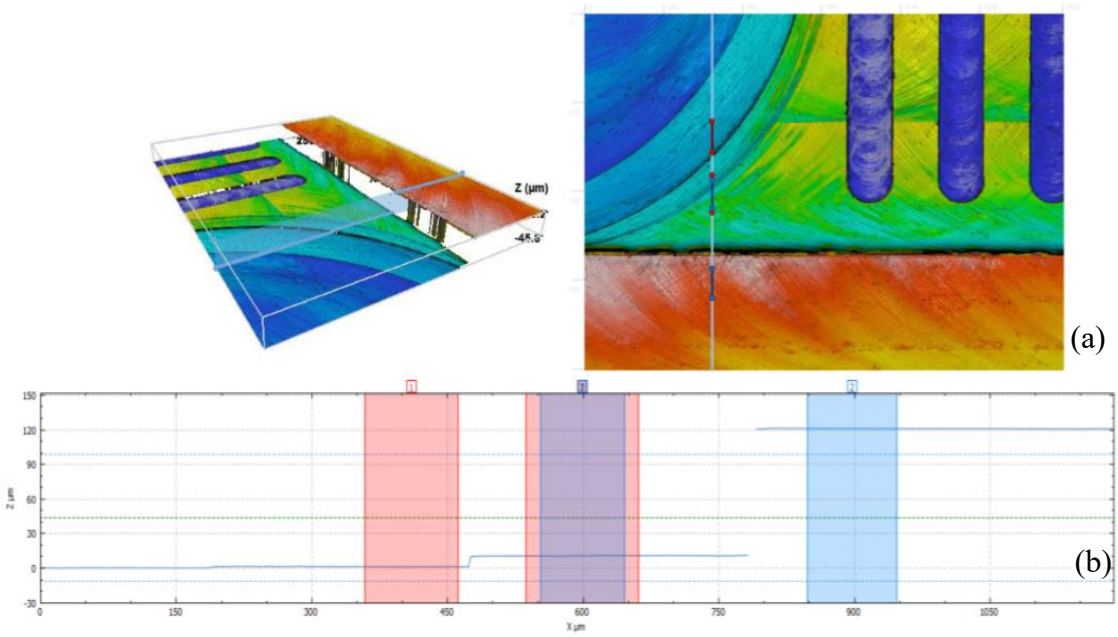

Figure 3.15 *(a) 3D view of the interest area. (b) Results of the profilometric analysis to quantify the relative height between the lateral chamber and the outer region.*

The profilometric plot of the measure of the relative height between the lateral channel and the micro-channel is reported in Figure 3.16.

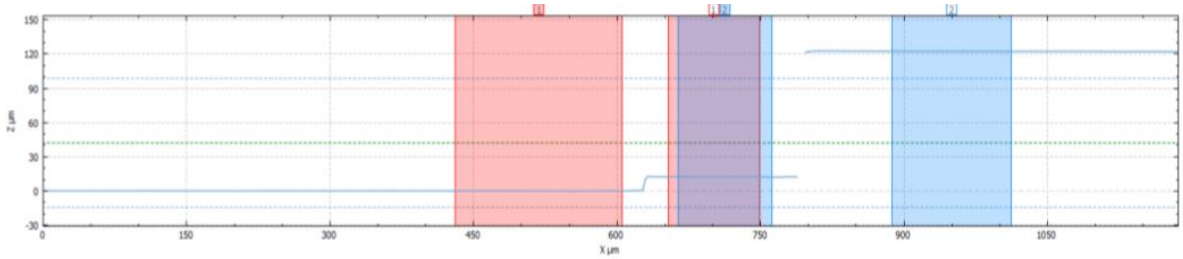

Figure 3.16 *Results of the profilometric analysis to quantify the relative height between the lateral channel and the micro-channel.*

Table ***3.11*** shows the results for area C.

Table 3.11 *Results of the profilometric anaysis for area C.*

Measure region	Design value [µm]	Measured value [µm]
Height of the micro-channel	10.00	12.34
Central chamber vs outer region	120.00	119.80
Central chamber vs micro-channel	110	110.08

From these results, it can be said that micromilling is a suitable technique to produce masters for microfluidic devices.

The only limitation of this technique involves the tools used in the micromilling of the mold; the head mills must be substituted often, as soon as they show signs of wear, to avoid the presence of differences between the real and the design values. This procedure can increase a lot the cost of the process and the procedure time.

3.1.3 Production of the PDMS micro-bioreactor

The procedure described in §2.1.5 allows the production of the PDMS µ-bioreactor.

No problem is encountered during this operation; moreover, the removal of the cured PDMS layer from the master is easy and does not leave any residues. This demonstrates that the aluminum is compatible with PDMS and allows a good reticulation keeping unchanged the final properties of the PDMS.

3.1.4 Irreversible configuration

The procedure in paragraph §2.1.6 allows to build the final irreversible configuration of the µ-bioreactor, shown in Figure 3.17 where the platform is filled with food coloring to better visualize its geometry.

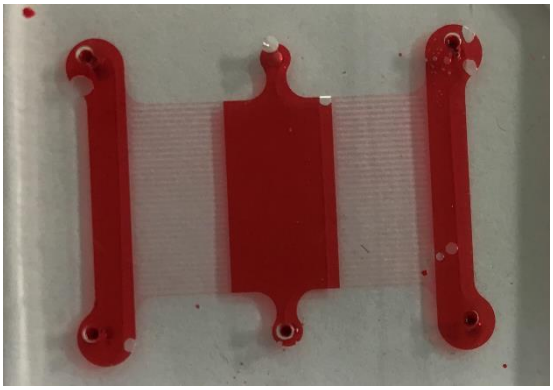

Figure 3.17 *Micro-bioreactor full filled with colour to better visualize its shape.*

3.1.5 Validation experiments

In order to obtain qualitative and quantitative data about the performances of the microfluidic device, validation experiments are conducted as described in paragraph §2.1.8.1. Food coloring and fluorescent isothiocyanate-dextrans are prepared and used in these experiments. The fluorescent tracer with the highest molecular weight is used in order to obtain results comparable to and representative of the behavior of exosomes inside the micro-bioreactor.

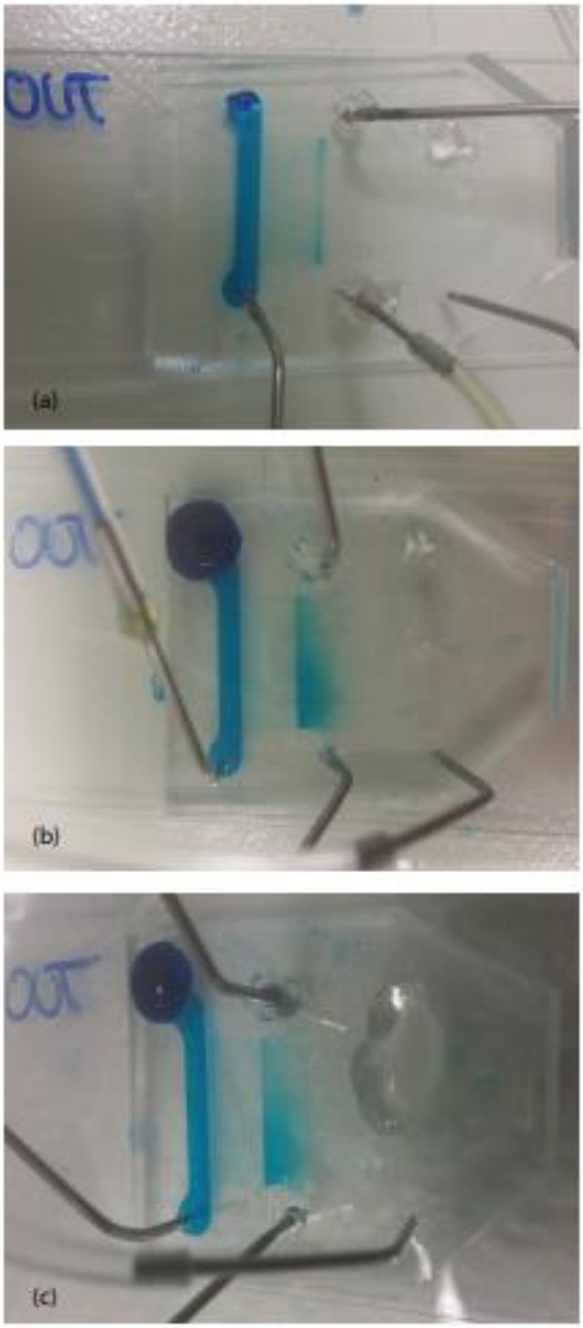

Figure 3.18 *Result of the validation experiment with food colouring on the irreversible configuration. Picture are taken (a) at the beginning of the experiment, (b) after 30 minutes and (c) after 24 hours to verify if the steady state is maintained.*

First, the food coloring is used to obtain qualitative information about the performances of the device. The syringe pump is set up by placing the two syringes on the infuse. The syringes are prepared and placed on the pump, which is then started. The flow rate is set on the pump display, usually between 5 and 15 µL/min to favor the establishment of the steady state.

After approximately 30 minutes the device reaches the steady state.

Figure 3.18 shows the result of the food coloring validation experiment. Picture are taken at different times after the beginning of the experiment to understand how much time does the steady state take need to be achieved and if it is maintained for 24 hours.

Based on the image in Figure 3.18, the fluids enter the bottom side and exit via the top side. The right hand channel is connected with the syringe containing the food coloring solution, while the right hand one is filled with water. The central chamber is characterized by the presence of the concentration gradient, as it can be observed from the picture. Visually, the color tends to lighten from an intense blue to transparent, meaning that the concentration of food coloring in water is decreasing.

This experiment shows the desired result, i.e. the formation of a concentration gradient across the central chamber. However, this is only a qualitative information.

The next step is the use of fluorescent isothiocyanate-dextrans to obtain semi-quantitative data, thanks to the fluorescence microscope. All the data reported refer to the dextran with the highest molecular weight (500kDa), that has the nearest diffusion coefficient with respect to the exosomes. During these experiments, the pump is prepared and started with the same method used in the previous case. However, now it is necessary to wrap the syringe containing the fluorescent tracer, the micro-tubes and the µ-bioreactor with aluminum foil to protect them from light. Since fluorescent dextrans are light sensible, this procedure is necessary to ensure the stability of the solution.

During these experiments, the µ-bioreactor is placed and kept on the microscope stage, to avoid an excessive movement that can create turbulences inside the platform. Therefore, images can be taken with the fluorescence microscope (GFP Cube), combined and analyzed with ImageJ. Figure 3.19 shows an image of a section of the µ-bioreactor. Both lateral channels, micro-channels and the central chamber are represented.

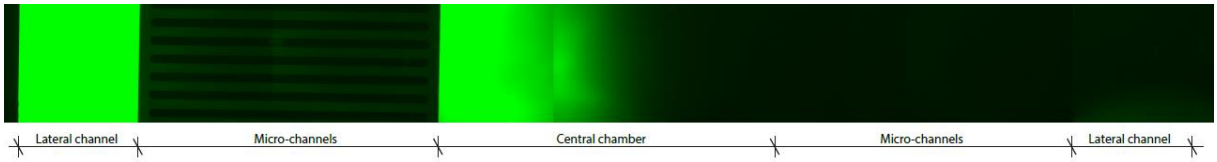

Figure 3.19 *Result of the validation experiment with high MW fluorescent isothiocyanate-dextran on the irreversible configuration of the micro-bioreactor.*

The presence of the concentration gradient can be easily observed. Moreover, it is possible to load the image in ImageJ and measure the light intensity inside the central chamber,

considering 7 representative areas. Values are normalized to a 0 to 1 scale with respect to the highest intensity value. The results can be compared with normalized concentration values of the COMSOL Multiphysics® simulation. It is not expected to have a perfect correspondence, since in the simulation the convective flux is manually set to zero. However, this procedure is useful to obtain a quantitative comparison with the simulation. The following graph, Figure 3.20, shows the difference between theoretical and

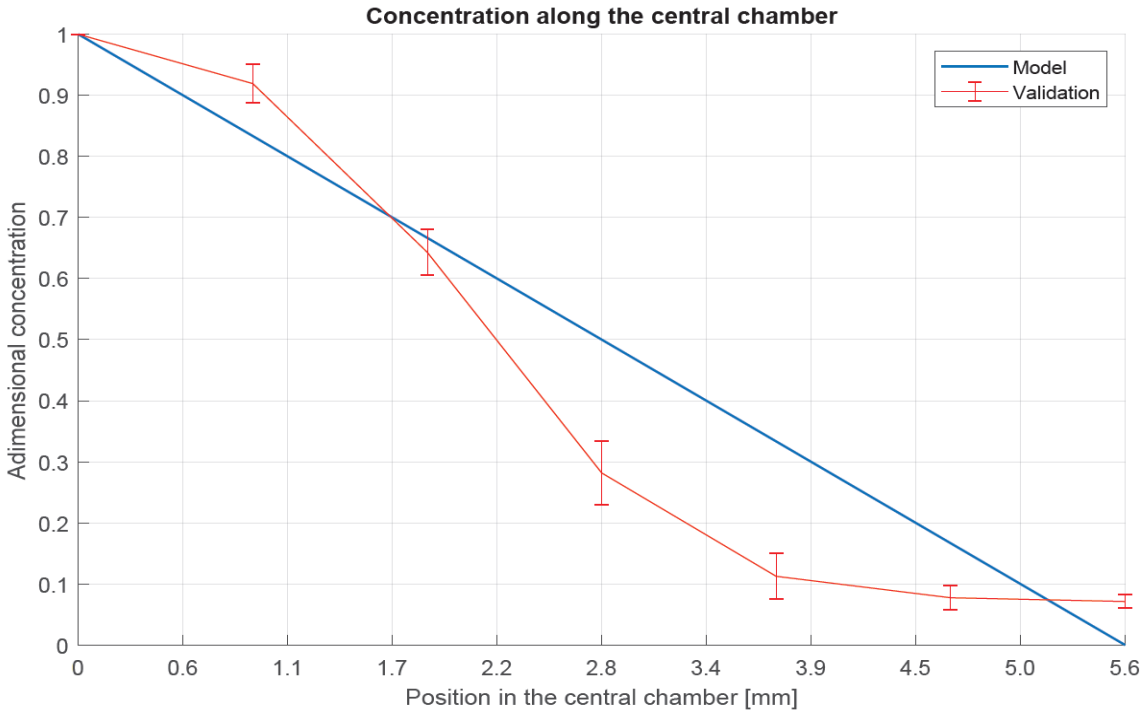

Figure 3.20 *Difference between the theoretical normalized concentration values and the experimental values, obtained from different experiments with dextrans.*

experimental values.

The experimental data are in good agreement with the theoretical values. The measurement error (standard deviation on 12 data points), tends to increase in the central region of the culture chamber. This can be explained considering that the measurement of the light intensity with ImageJ® is not an extremely precise method, and an error is expected from this type of measure.

It can be stated that the performances of the μ-bioreactor arranged in the irreversible configuration are validated, since it shows the desired and expected trend of concentration.

3.2.6 Biological experiments

The μ-bioreactor produced is used in its irreversible configuration to perform some biological tests, in order to define a procedure for the injection of cells and to observe the cell viability. The device is prepared for the biological experiment as described in paragraph §2.1.9. The day after the cell seeding, the condition of cells in the central

chamber should be similar to Figure 3.21, where cells are attached to the surface, alive and not clustering.

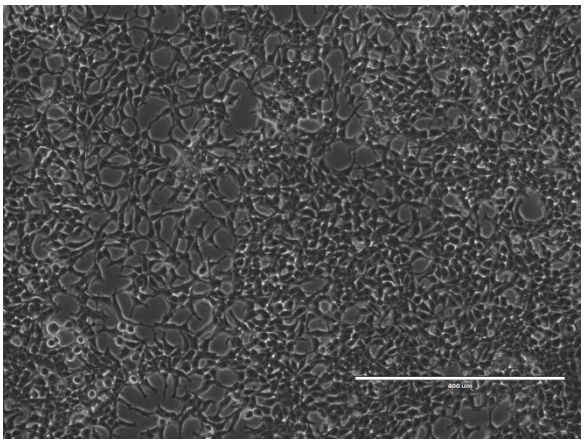

Figure 3.21 *Theoretical aspect of the cells attached to the surface of the central chamber 24 hours after the seeding.*

Some problems arose during these biological experiments. After the seeding procedure the cells do not seem to properly attach to the central chamber's surface.

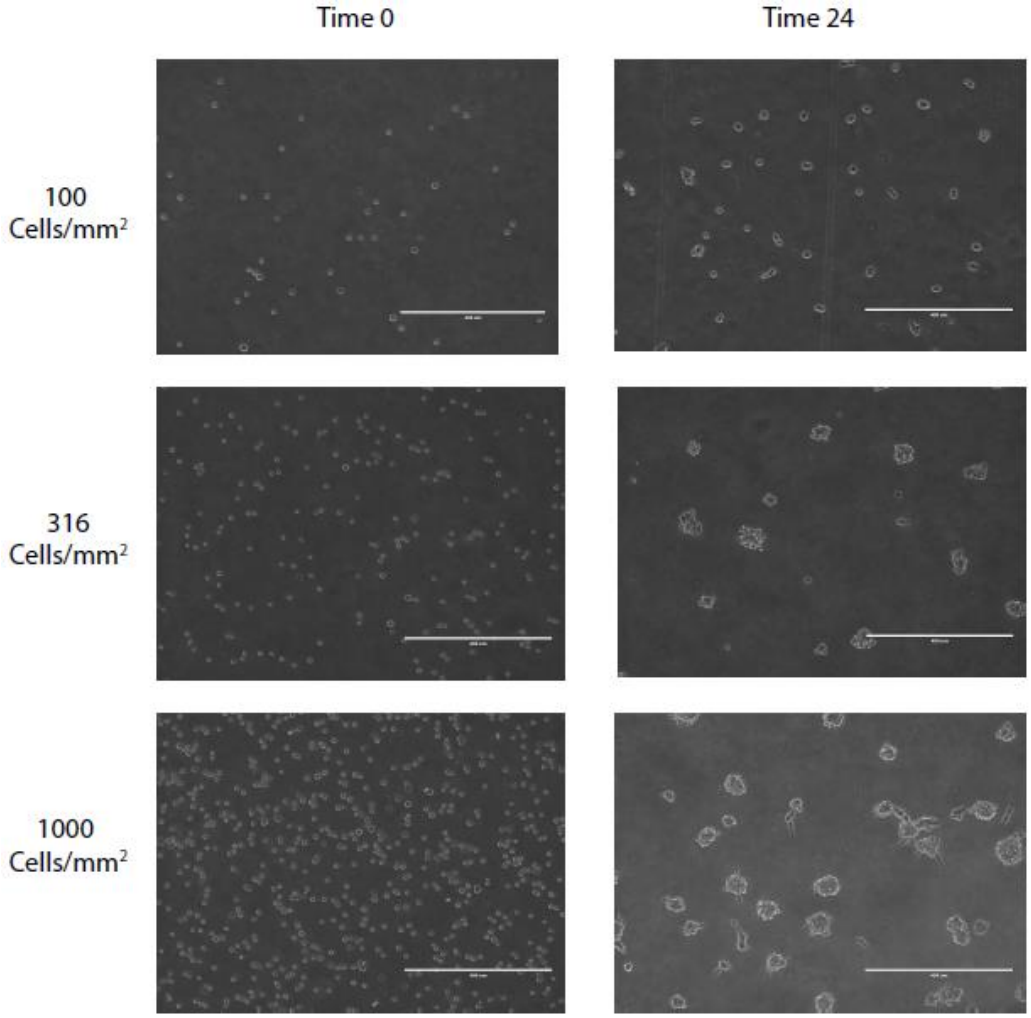

Figure 3.22 *Pictures of the cells inside the μ-bioreactor at different concentration and at time 0 and time 24.*

Experiments at different concentrations of cells in the seeding solution are carried out, but all of them show the same results. Figure 3.22 shows some pictures at three concentration of cells that differs of half a log one from the other; images are reported at time 0 and time 24 hours.

In the second column it can be noticed that the cells tend to cluster, maybe because the volume of medium inside the central chamber (6.72 μL) is not enough to keep them alive. This theory is confirmed by looking at the regions near the seeding doors, where the supply of nutrients is ensured by the volume of culture medium presence inside and above the seeding hole.

Figure 3.23 shows some cells 24 hours after the seeding in proximity of the seeding door.

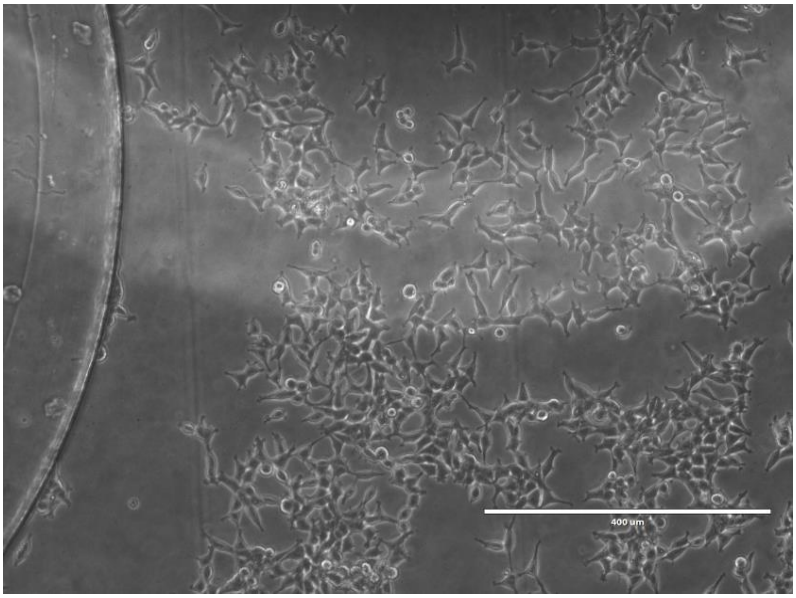

Figure 3.23 *Cells attached to the central chamber surface in proximity of the seeding door. Cells are seeded with a concentration of 1000 cells/mm^2.*

The picture refers to a micro-bioreactor seeded with a concentration of 1000 cells/mm^2.

To solve this problem, it would be necessary to increase the height of the central chamber to provide a larger volume of culture medium available for the proper survival of the cells.

To obtain more evidence of this theory, the actual micro-bioreactor is modified adding a thin layer of PDMS (height of 250 μm) pierced in correspondence of the central chamber. This layer is irreversibly attached through a two step plasma treatment between the micro-bioreactor and the glass slide. The new and the old dimensions of the central chamber are reported in Table 3.12.

Table 3.12 *New and old dimensions of the micro-bioreactor central chamber.*

Dimensions		Old values	New values
Width of the central chamber	[mm]	5.60	5.60
Height of the central chamber	[mm]	0.12	0.37
Length of the central chamber	[mm]	10.00	10.00
Surface of the central chamber	[mm^2]	56.00	56.00
Volume of the central chamber	[mm^3]	6.72	20.72

The experimental procedure is the same as one described above and pictures just after the seeding procedure (Figure 3.24*a*) and after 24 hours (Figure 3.24*b*) are captured.

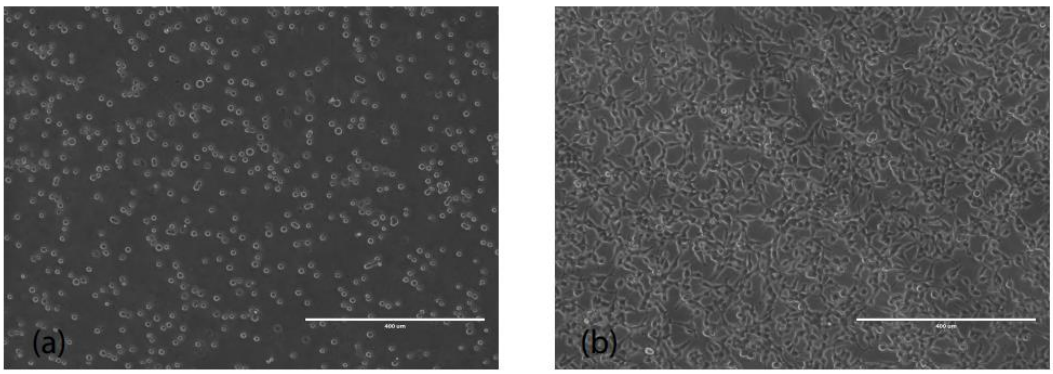

Figure 3.24 *Pictures of the central chamber seeded. (a) Cells seeded at time zero and (b) cells completely attached after 24 hours. The concentration of cells seeded is 1000 cells/mm^2.*

It is clear how the cells are completely attached to the bottom surface of the central chamber; the entire surface is completely covered by cells and, once attached, the culture medium could be refreshed by gently removing the old medium with a micropipette and consequently injecting 21 µm of fresh medium.

To verify the viability of the cells inside the central chamber, the µ-bioreactor is washed with DMEM (without FBS) and then completely filled with the staining solution containing Hoechst and Calceine AM. Hoechst dye stains all nuclei blue, while Calceine AM stains the cytoplasm of live cells giving a bright green fluorescent signal. The solutions of Hoechst and Calceine AM are prepared following the procedure described in §2.1.9. The stain solution is left inside the chamber for 45 minutes; the µ-bioreactor is covered with aluminum foil to protect the stain solution from the light.

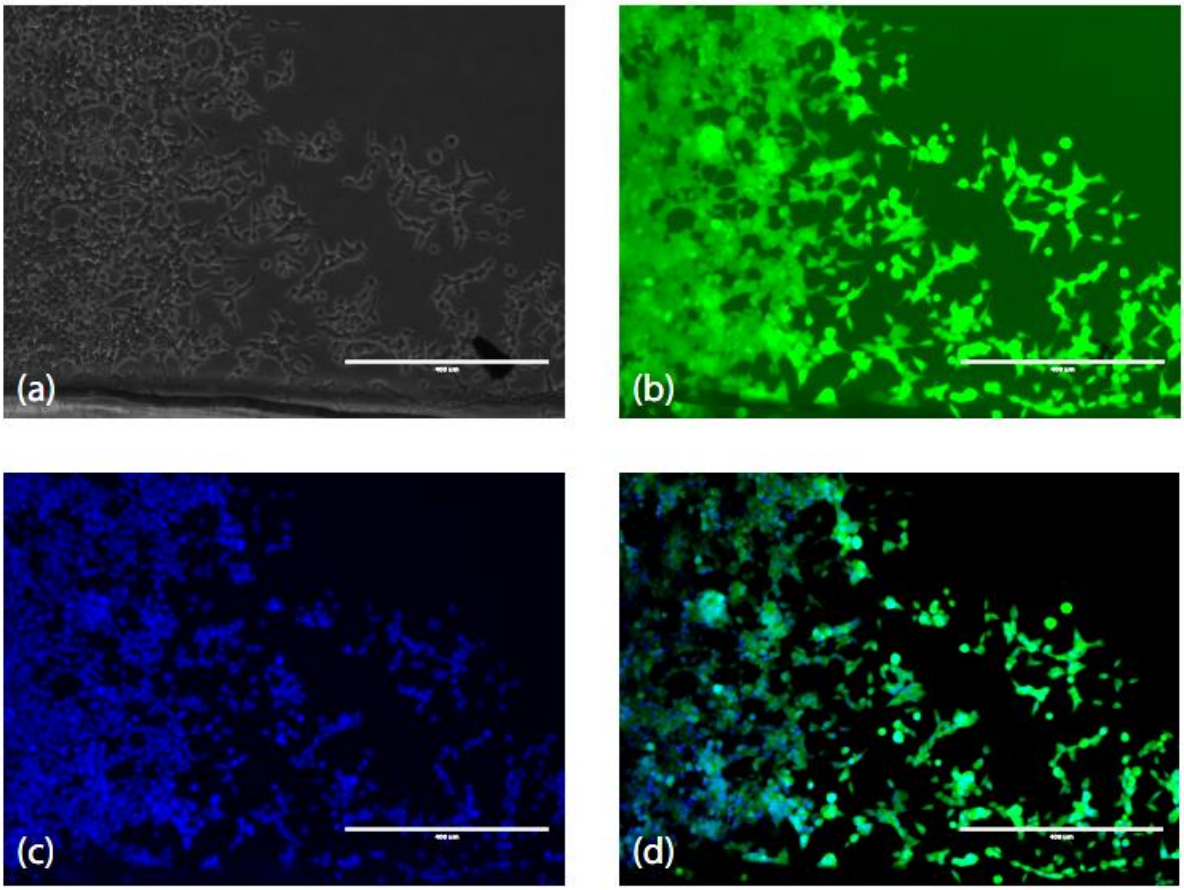

Figure 3.25 *Fluorescence acquisitions of the central chamber of the μ-bioreactor during the Hoechst and Calceine AM stain; the stain is carried out 24 hours after the cells seeding.. (a) The cells view in bright field. (b) Calcein-AM stain that highlights the cytoplasm. (c) Hoechst stain that highlights the cells' nuclei. (d) Overlay od Hoechst and Calceine AM images.*

Figure 3.25*a* shows a bright field image of the central chamber covered by cells. Figure 3.25*b* hows a fluorescence acquisition the central chamber with the GFP cube, showing viable cells' cytoplasm highlighted by Calcein-AM. Figure 3.25*c,* taken with the DAPI cube, highlights the nuclei of all cells stained with the Hoechst dye. An overlay of the two images is shown in Figure 3.25*d*.

Even if the cells survival problem is overcome, further studies are needed to verify if the steady state concentration gradient inside the central chamber is achieved. The main limitations could be the presence of the thin layer of PDMS between the μ-bioreactor and the glass slides and the tripled height of the central chamber. The first one can imply the collapse of the micro-channels during the plasma bonding; this inconvenient could reduce the number of channels available for the mass transport of the substance that should diffuse. The second problem could generate a non-homogenous distribution of particles along the height direction of the central chamber.

3.2 Reversible configuration

3.2.1 Design of the reversible configuration

The structure will be composed, from bottom to top, by the following (Figure 3.26):

- A glass slide 76x26 mm;
- A PDMS casing layer with a slab carved to accommodate a circular glass coverslip. This membrane is irreversibly attached to (i) by plasma treatment;
- A PDMS vacuum layer with a circular cavity, the vacuum membrane, that allows the reversible sealing of (i) and (ii).

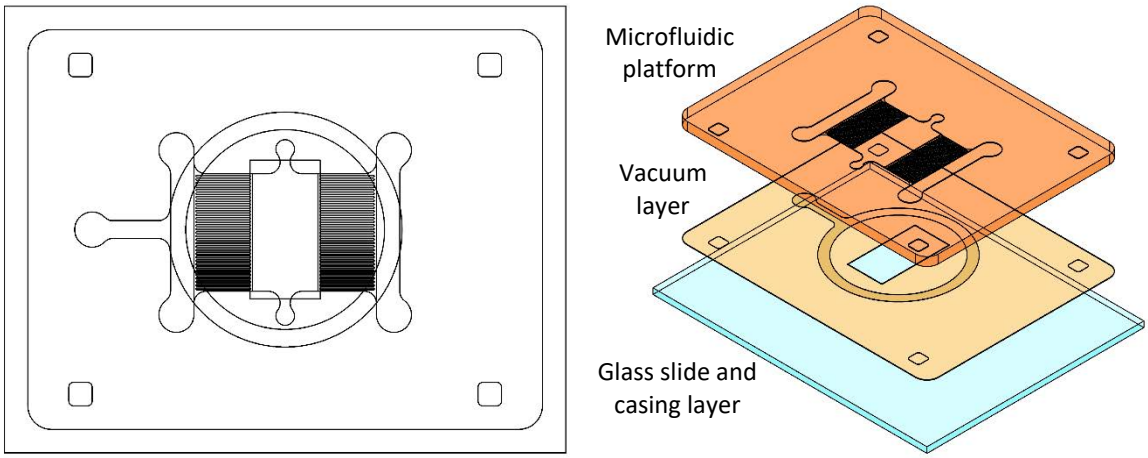

Figure 3.26 *Top (a) and isometric (b) view of the vacuum system used to create the reversible hydraulic seal between the microfluidic platform and the glass slide.*

Here the design of the reversible configuration is presented. Both casing layer and vacuum layer are included inside a rectangle: its function is to easily cut the PDMS in excess and to obtain two slices that can be aligned between themselves and with the support glass slide. The vacuum layer design involves the presence of the same alignment marks that are present on the micro-bioreactor; this allows the perfect alignment between the two structures.

The design of both layers is shown in Figure 3.27.

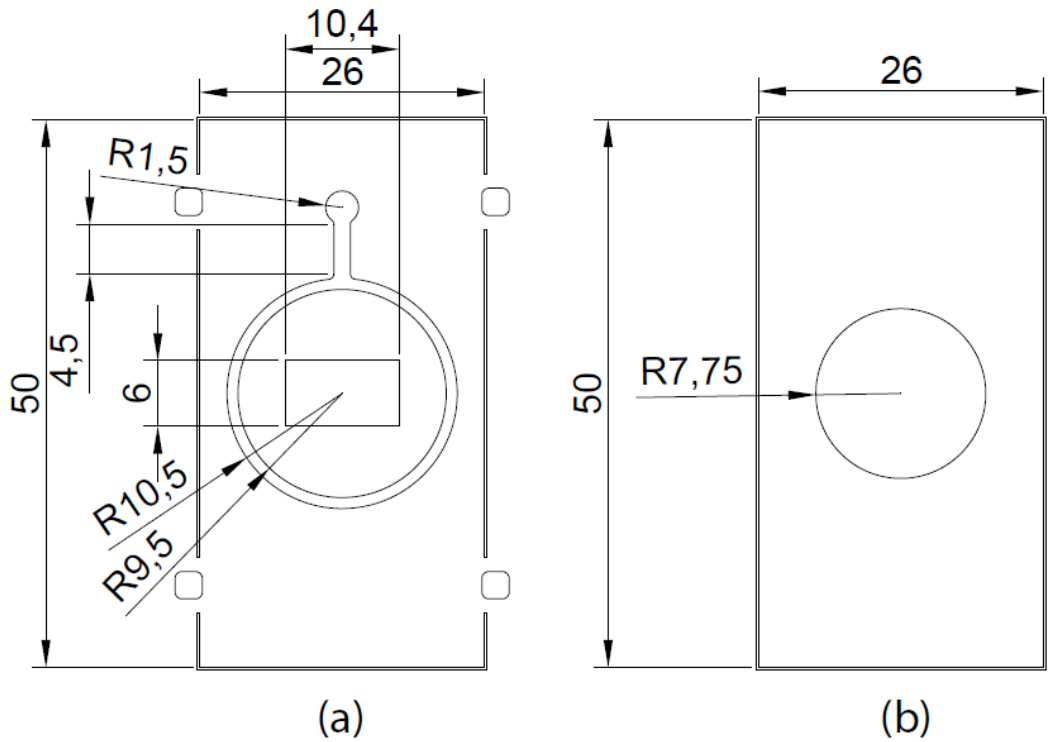

Figure 3.27 *(a) Design of the vacuum layer and (b) of the casing layer.*

3.2.2 Production of the casing layer and of the vacuum layer masters

The masters are produced as describe in §2.1.7.1 and §2.1.7.2.

Figure 3.28 shows the two final masters.

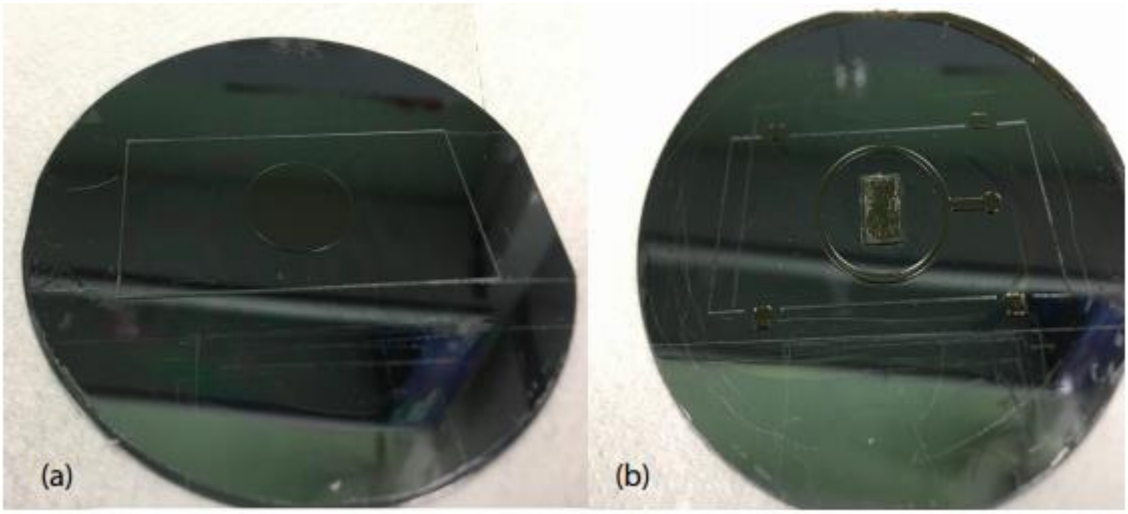

Figure 3.28 (*a) Master of the casing layer and (b) of the vacuum layer.*

3.2.3 Production of the casing layer and of the vacuum layer in PDMS

The procedure in paragraph §2.1.7.4 allows to build the final reversible configuration. The casing layer is produced and assembled with the support glass slide (figure Figure 3.29*a*); the vacuum layer is constructed and irreversibly attached to the micro-bioreactor layer (Figure 3.29*b*).

The alignment of the structure turns out to be an easy procedure, thanks to the alignment

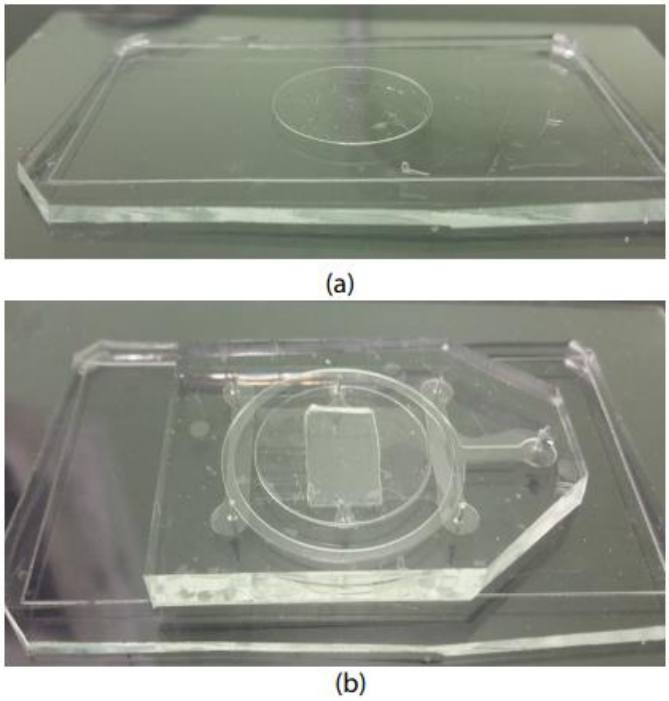

Figure 3.29 *(a) The casing layer assembled with the support glass slide. (b) The vacuum layer constructed and irreversibly attached to the micro-bioreactor layer.*

marks and to the cutting lines presented in all the layers involved.

Some problems arose during the attachment of the μ-bioreactor to the vacuum layer: this procedure must be carried out with care to avoid the collapse of the micro-channels over the PDMS of the vacuum layer.

3.2.4 Production of the vacuum control plant

The vacuum plant is formed by:

- A small vacuum pump (Figure 3.31 in red)
- An electro valve controlled by a digital vacuum switch Figure 3.31 in purple)
- A surge tank to collect any possible trace of fluid sucked from the vacuum system Figure 3.31 in yellow)
- A vacuum pipe to connect the vacuum plant to the vacuum system.

Figure 3.31 shows the vacuum system assembled in BIAMET laboratory.

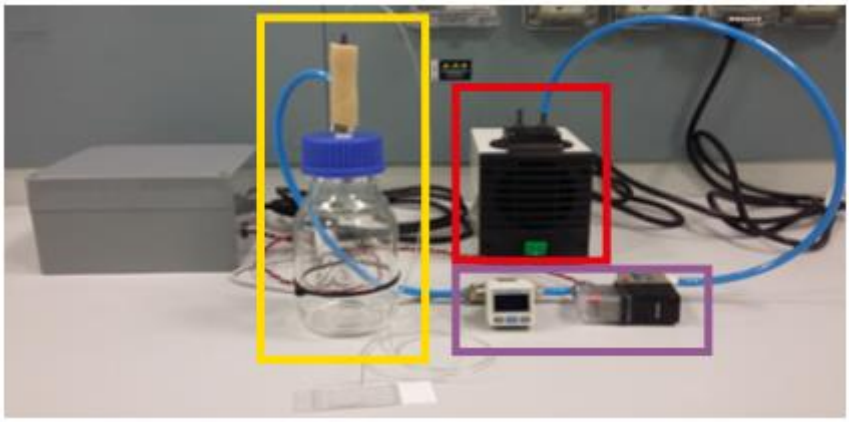

Figure 3.31 *Vacuum plant assembled in BIAMET laboratory. Following the blue pipe, from right to left: the vacuum pump, the electrovalve, the digital vacuum switch, the surge tank and the yellow vacuum pipe.*

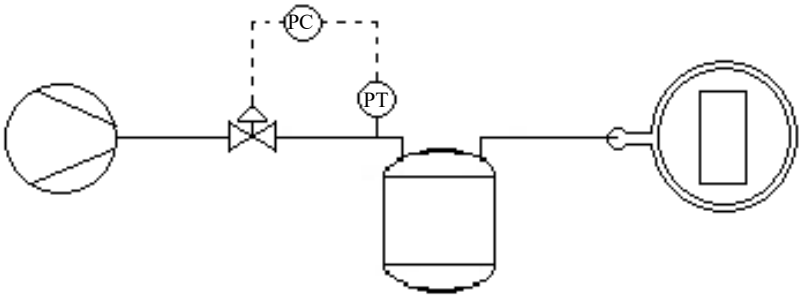

Figure 3.30 *Control scheme of the vacuum plant*

Operatively, when the pump is switched on, the vacuum switch sends a signal to the electro valve, which can be fully open or fully closed. When the pressure inside the vacuum system is below the set point, the valve is fully closed, when the pressure inside the vacuum system goes above the set point, the valve fully opens until the pressure is under the set point again, than the valve is closed again. Figure 3.30 shows the control scheme of the vacuum plant.

3.2.4 Hydraulic seal of the reversible configuration

The hydraulic seal of the reversible configuration is validated following the procedure presented in §2.1.8.2. Unfortunately, the validation experiment gave only partially positive result.

10 minutes after the fluid starts flowing inside the μ-bioreactor, the vacuum system laminates and the fluid exits from the central chamber. Figure 3.32*a* shows the vacuum system working correctly in the first minutes of operation, the μ-bioreactor is full filled with red food coloring to instantaneously discover any fluid loses; Figure 3.32*b* shows the lamination process.

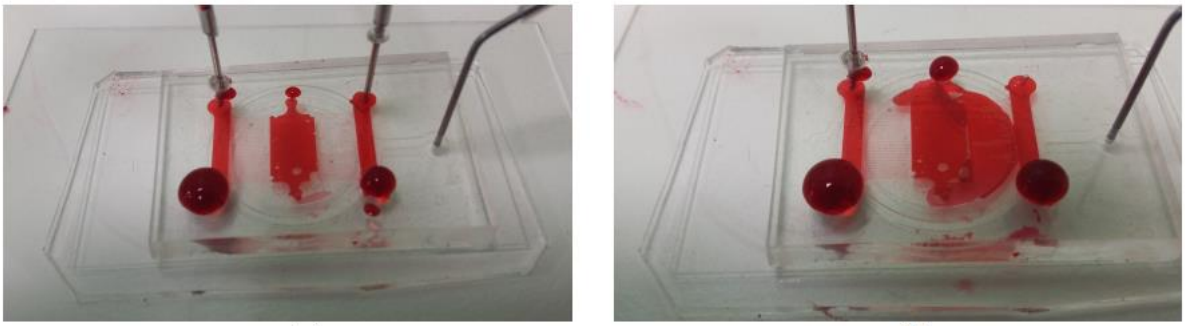

Figure 3.32 *(a) Vacuum system working properly. (b) Lamination process of the device.*

The dimensions of the vacuum suction ring seems to be too small so the hydraulic seal is not ensured. To solve this problem the design of the vacuum layer must be improved. The dimension of the vacuum suction ring should be increase to ensure the achievement of a higher vacuum force, to permit the reversible attachment of the two micro-bioreactor to the casing layer through the vacuum.

An idea for a new design of the vacuum layer is presented in Figure 3.33.

Even if further studies should be carried out to investigate whether this new system absolves its purpose or not, it is clear that the reversible configuration could improve the functionality of the µ-bioreactor. The new silicon master should be produced via photo-lithography and the new system should be product and validate to verify its hydraulic seal.

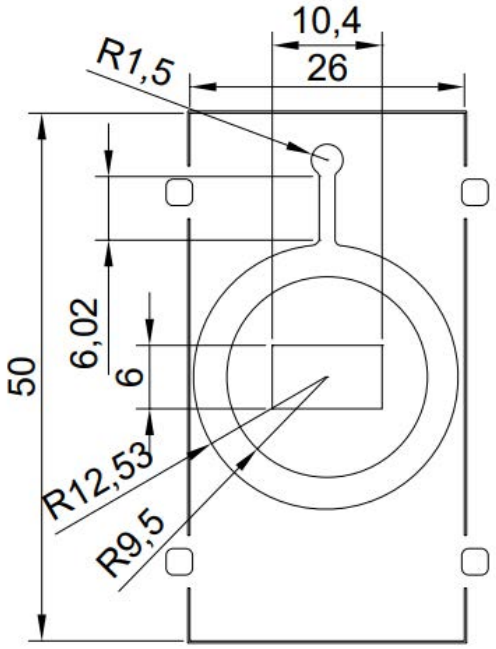

Figure 3.33 *New design of the vacuum layer.*

Conclusions

The objective of this work of thesis was the study and development a microfluidic platform for biomedical applications that was able to improve upon typical limitations of *in vitro* cultures, such as the inability of recreating the complex cellular microenvironment that characterizes the *in vivo* cultures.

A micro-bioreactor has been designed and optimized, with the aim of reproducing a continuous concentration gradient inside its central chamber. This device will be used to investigate the behaviour of exosomes, cellular vesicles, identified as biomarkers, on the metastatic diffusion of Neuroblastoma, an aggressive childhood tumour. The purpose was to discover how cells react at different exosomes concentrations, and whether cells internalize them or not.

The design of the micro-bioreactor started from an existing device that failed to create the requested concentration gradient inside its central chamber. After some geometrical modifications, the most important related to the micro-channels dimensions, some fluid dynamic simulations have been carried out. These simulations confirmed that the new design is suitable to create a stable concentration gradient. Then, the new platform's master was produced in aluminum with a micromiller. The micro-bioreactor obtained via replica molding process in PDMS was tested in its irreversible configuration, first using food coloring and then fluxing a fluorescent dextran solution. Both experiments confirm the presence of a stable concentration gradient inside the central chamber. No significant problems arose during these first part but it has been noticed that the device assembling procedure must be carried out with great care, in order to avoid the structural collapse of the micro-channels over the glass slide.

The device was then used for some biological experiments. Some HEK-293 cells were cultured inside the central chamber but it has been discovered that the volume of culture media present was not sufficient to maintain them alive. To overcome this problem some test have been carried out; it has been observed that increasing the chamber height from 120 microns to 370 microns, the cells can be easily cultured and maintained alive for more than 48 hours. To verify the cells viability, the micro-bioreactor was tested with Hoechst and Calceine AM stain solution: the first one highlights the cells nuclei while the second one marks the cytoplasm of live cells. The result was that the cells were perfectly still alive after 48 hours from their seeding. Moreover, once attached to the internal surface of the micro-bioreactor, the cells cannot be easily removed so culture medium can be replaced with the help of a manual micropipette, to guarantee the correct concentration of nutrients for the cells growth.

A parallel project involved the creation of a reversible configuration that would enable to easily remove the cells from the central chamber to perform further post processing analyses. A vacuum system has been studied, formed by two thin PDMS layer. The first one, called casing layer, has the function of creating the right place for positioning a circular coverslip, where cells can be seeded. The second one, called vacuum layer, is irreversibly attached to the micro-bioreactor; this layer is equipped with a rectangular hole in correspondence with the central chamber and a sort of circular channel used to reversibly attach the micro-bioreactor to the casing layer. Then, a vacuum plant has been developed to ensure the correct vacuum degree between the casing layer and the micro-bioreactor. It has been proved that the designed system, produced via soft lithography on PDMS, was not able to ensure the hydraulic seal of the platform, maybe because of the very small dimensions of the vacuum suction ring present over the vacuum layer. To solve this problem, a new design for the vacuum layer has been developed and the dimensions of the vacuum suction ring have been increased.

To conclude, the micro-bioreactor is suitable to obtain continuous concentration gradients inside its central chamber. However, in future studies, the central chamber height should be increased, to ensure optimal culture conditions for cells seeded inside it. The vacuum system should be modified following the suggested new design, in order to obtain the reversible configuration, ensuring the hydraulic seal between the casing and the vacuum layer.

Nomenclature

c	=	concentration [mol/m^3]
Ca	=	capillary number [dimensionless]
D	=	diameter [m]
D_{eq}	=	equivalent diameter [m]
D_i	=	diffusion coefficient of the species i [m^2/s]
f	=	friction factor [dimensionless]
h	=	height of the channel [m]
J_i	=	diffusive flux of the species i [mol/s]
k_B	=	Boltzmann constant [J/K]
L	=	length of the channel [m]
L_{eq}	=	Equivalent length in the equivalent diameter method [m]
N	=	number of cells per mL [cells/mL]
N_0	=	initial number of cells
$n_{i,eq}$	=	coefficient of the equivalent diameter method [dimensionless]
N_{mean}	=	mean number of cells [cells/square]
N_{tot}	=	total number of cells
P	=	semiperimeter [m]
Pe	=	Péclet number [dimensionless]
r	=	radius [m]
Re	=	Reynolds number [dimensionless]
S	=	section of the channel [m^2]
T	=	temperature [K]
V	=	average velocity [m/s]
v	=	velocity [m/s]
w	=	width of the channel [m]
ΔP	=	pressure drops [Pa]

Greek symbols

μ*BR*	=	microbioreactor
DMEM	=	Dulbecco's Modified Eagle Medium
DMSO	=	Dimethyl sulfoxide
FBS	=	Fetal Bovine Serum
PBS	=	Phosphate Buffered Saline
PDMS	=	Polydimethylsiloxane

Acronyms

μ	=	viscosity [Pa·s]
γ	=	surface tension [N]
η	=	mobility of the particle [kg/s]
ρ	=	density [kg/m^3]

Appendix

A.1 Photomasks

In this section are represented the photomasks used in the photolithography technology to produce the masters of the casing layer and of the vacuum layer.

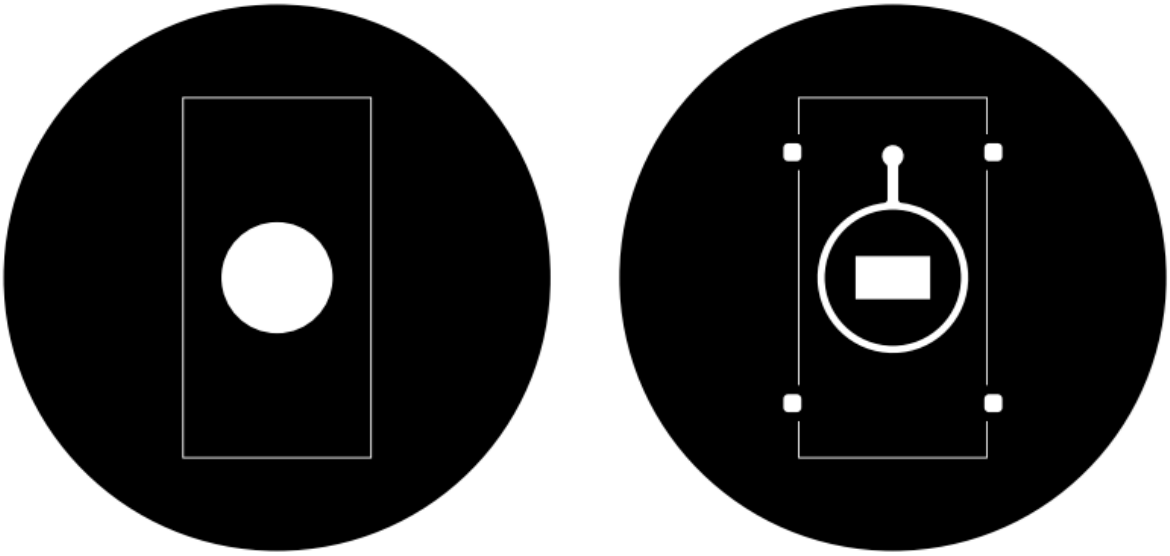

Figure A.1 *(a) Photomask of the casing layer and (b) of the vacuum layer.*

A.2 Equivalent diameters method

The procedure used to calculate the equivalent length of the microchannels using the method of the equivalent diameters is here presented.
It is needed to add two angles of 45° at the inlet and outlet of the microchannels, and three 90° elbows along the channels, as presented in Figure 3.3. The length of each microchannel is calculated using trigonometric relations and it is equal to 5871.14 µm.
The elbow added can be assimilated to concentrated pressure drop point that can be converted into additional lengths, considering the equivalent diameters method.

$$L_{eq} = D_{eq} \sum n_{i,eq}, \qquad \text{(A.1)}$$

where L_{eq} is the equivalent length [μm], D_{eq} is the equivalent diameter [μm] and $n_{i,eq}$ is a coefficient that is correlated to the type of elbow used (15 for the 45° elbow, 35 for the 90° elbow). So, adding two 45° elbows and three 90° elbows, the result is:

$$n_{i,eqTOT} = 2 \cdot 15 + 3 \cdot 35 = 135 \tag{A.2}$$

$$L_{eq} = 2531.25\ \mu m \tag{A.3}$$

The total length of each microchannel can be calculated as:

$$L_{TOT} = L + L_{eq} = 8402.39\ \mu m \tag{A.4}$$

This value is used in the Fanning equation to calculate the velocity as:

$$v = \frac{D_{eq}^2 \cdot \Delta P}{32 \cdot \mu \cdot L_{TOT}} \tag{A.5}$$

References

[1] G. M. Whitesides, “The origins and the future of microfluidics,” *Nature*, vol. 442, no. 7101, pp. 368–373, Jul. 2006.

[2] T. M. Squires and S. R. Quake, “Microfluidics: Fluid physics at the nanoliter scale,” *Rev. Mod. Phys.*, vol. 77, no. 3, pp. 977–1026, Oct. 2005.

[3] E. K. Sackmann, A. L. Fulton, and D. J. Beebe, “The present and future role of microfluidics in biomedical research,” *Nature*, vol. 507, no. 7491, pp. 181–189, Mar. 2014.

[4] T. A. Duncombe, A. M. Tentori, and A. E. Herr, “Microfluidics: Reframing biological enquiry,” *Nat. Rev. Mol. Cell Biol.*, vol. 16, no. 9, pp. 554–567, 2015.

[5] M. Mehling and S. Tay, “Microfluidic cell culture,” *Curr. Opin. Biotechnol.*, vol. 25, pp. 95–102, 2014.

[6] D. N. Breslauer, P. J. Lee, and L. P. Lee, “Microfluidics-based systems biology,” *Mol. Biosyst.*, vol. 2, no. 2, pp. 97–112, 2006.

[7] E. Cimetta *et al.*, “Microfluidic bioreactor for dynamic regulation of early mesodermal commitment in human pluripotent stem cells.,” *Lab Chip*, vol. 13, no. 3, pp. 355–64, Feb. 2013.

[8] D. J. Beebe, G. A. Mensing, and G. M. Walker, “Physics and Applications of Microfluidics in Biology,” *Annu. Rev. Biomed. Eng.*, vol. 4, no. 1, pp. 261–286, 2002.

[9] S. Halldorsson, E. Lucumi, R. Gómez-Sjöberg, and R. M. T. Fleming, “Advantages and challenges of microfluidic cell culture in polydimethylsiloxane devices,” *Biosens. Bioelectron.*, vol. 63, pp. 218–231, 2015.

[10] I. D. Johnston, D. K. McCluskey, C. K. L. Tan, and M. C. Tracey, “Mechanical characterization of bulk Sylgard 184 for microfluidics and microengineering,” *J. Micromechanics Microengineering*, vol. 24, no. 3, 2014.

[11] “Plasma Surface Treatment | Harrick Plasma.” [Online]. Available: http://harrickplasma.com/plasma/plasma-surface-treatment. [Accessed: 10-Jan-2019].

[12] “Physics | Harrick Plasma.” [Online]. Available: http://harrickplasma.com/plasma/physics. [Accessed: 10-Jan-2019].

[13] “PDMS Soft lithography : Plasma cleaner - Elveflow.” [Online]. Available: https://www.elveflow.com/microfluidic-tutorials/soft-lithography-reviews-and-tutorials/how-to-choose-your-soft-lithography-instruments/pdms-soft-lithography-plasma-cleaner/. [Accessed: 10-Jan-2019].

[14] K. De Preter *et al.*, “Open Access Human fetal neuroblast and neuroblastoma transcriptome analysis confirms neuroblast origin and highlights neuroblastoma candidate genes,” *Genome Biol.*, 2006.

[15] A. Thind and C. Wilson, “Exosomal miRNAs as cancer biomarkers and therapeutic targets,” *J. Extracell. Vesicles*, vol. 5, no. 1, 2016.

[16] J. Caradec, G. Kharmate, E. Hosseini-Beheshti, H. Adomat, M. Gleave, and E. Guns, “Reproducibility and efficiency of serum-derived exosome extraction methods,” *Clin. Biochem.*, vol. 47, no. 13–14, pp. 1286–1292, 2014.

[17] W. Li *et al.*, “Role of exosomal proteins in cancer diagnosis,” *Mol. Cancer*, vol. 16, no. 1, pp. 1–12, 2017.

[18] “Stanford University.” [Online]. Available: https://web.stanford.edu/group/foundry/Basic Design Rules.html. [Accessed: 14-Jan-2019].

[19] “MICROMASTER® 3/5X - KUGLER GmbH.” [Online]. Available: https://www.kugler-precision.com/index.php?MICROMASTER--3-5X-EN. [Accessed: 17-Jan-2019].

[20] “S neox - Non-contact 3D surface profiler.” [Online]. Available: https://www.sensofar.com/metrology/sneox/. [Accessed: 17-Jan-2019].

[21] P. Epoxy and N. Photoresist, “SU-8 2000 Permanent Epoxy Negative Photoresist

PROCESSING GUIDELINES FOR :," 2015.
[22] P. Epoxy and N. Photoresist, "SU-8 2000 Permanent Epoxy Negative Photoresist PROCESSING GUIDELINES FOR :," 2000.
[23] Sigma, "Dextran Molecular Weight," pp. 9–11.
[24] "Hoechst 33342 Protocol for Imaging - IT."
[25] "Introduction about soft-lithography for microfluidics - Elveflow." [Online]. Available: https://www.elveflow.com/microfluidic-tutorials/soft-lithography-reviews-and-tutorials/introduction-in-soft-lithography/introduction-about-soft-lithography-and-polymer-molding-for-microfluidic/. [Accessed: 10-Jan-2019].
[26] "PDMS: A review - Elveflow." [Online]. Available: https://www.elveflow.com/microfluidic-tutorials /microfluidic-reviews-and-tutorials/the-poly-di-methyl-siloxane-pdms-and-microfluidics/. [Accessed: 10-Jan-2019].
[27] M. A. Lake *et al.*, "Microfluidic device design, fabrication, and testing protocols Version 1.1: Last edited on 9 July 2015."

Ebbene sì, quasi non ci credo, ma sono qui a scrivere queste righe a conclusione non solo di questo lavoro di tesi, ma anche di un importante capitolo della mia vita. Il raggiungimento di questo sudato traguardo rappresenta per me un morivo di immensa gioia e mi dà la conferma che, nella vita, se ci si pone degli obbiettivi, con tenacia e costanza è possibile raggiungerli. Devo essere sincero, non sempre è stato facile, molte volte l'ostacolo sembrava invalicabile, la tesi sembrava non finire, l'esame sembra non potersi superare; ma è grazie alle persone che mi hanno circondato, e che tutt'ora mi circondano, che sono giunto alla fine di questo percorso.

Desidero innanzitutto ringraziare la mia relatrice, la Professoressa Elisa Cimetta, che con dedizione, pazienza e competenza mi ha permesso di svolgere questo lavoro di tesi nel suo laboratorio di ricerca. Un particolare grazie va alla mia amica Giorgia la quale mi ha fatto muovere i primi passi in laboratorio e mi ha insegato tutto quello che mi serviva sapere, lasciandomi le redini del progetto che stava seguendo. Di certo non mi sarei divertito senza la mia compagna di avventure Giulia, con la quale ho potuto sperimentare il piacere del condividere idee, risate e lamenti quando nulla andava per il verso giusto.

Da ricordare il team del laboratorio BIAMET, Sara, e in particolare Rosaria e Pina per avermi accompagnato nel mondo della biologia, non solo sempre a disposizione per risolvere i miei numerosi dubbi riguardo la materia ma anche un punto di riferimento nei numerosi momenti di sconforto. Grazie ragazze per aver sempre intuito al volo quello che stavo pensando e provando e per avermi incoraggiato a non mollare.

Grazie a voi amici universitari, per aver condiviso gran parte di questo cammino, per gli spritz bevuti assieme, per i pasti rubati e per gli scleri più o meno quotidiani. La strada sarebbe stata molto più dura senza di voi.

Grazie ai miei coinquilini, presenti e passati, siete riusciti sempre a farmi sentire davvero a Casa.

Grazie Gabry per avermi sopportato e nutrito in questi mesi di tensione: scusa per le volte in cui ti ho trattato male.

Un grazie va anche ai miei colleghi di lavoro, a Luca, per gli anni passati al ristorante, a Natale, Pasqua e capodanno siete stati la mia famiglia. Se sono quello che sono è anche merito di questa esperienza.

Un grazie immenso a voi amici molvenesi, per tutti questi anni passati assieme (e per aver sopportato la mia crescente acidità). Seppur spesso non siamo fisicamente vicini, so che per me siete e sarete sempre un punto di riferimento per lamia vita, vi voglio bene.

Grazie nonna Lena per avermi sempre spronato a studiare, a perseguire i miei obbiettivi. Grazie per il tuo aiuto.

Infine, ma non per ultimi, voglio dire un enorme grazie alla mia famiglia, Fede, Mamma e papà. Siete sempre stati pronti per un consiglio (e anche qualche litigata), un aiuto (anche economico) e mai avete smesso di credere in me. Questo traguardo lo dedico a voi.